

1 **Surface water and groundwater: Unifying**
2 **conceptualization and quantification of the two “water**
3 **worlds”**

4
5
6 Brian Berkowitz¹, Erwin Zehe²

7
8 1. Department of Earth and Planetary Sciences, Weizmann Institute of Science, Rehovot
9 7610001, Israel

10 2. Karlsruhe Institute of Technology (KIT), Karlsruhe, Germany

11
12 *Correspondence to:* Brian Berkowitz (brian.berkowitz@weizmann.ac.il)

13
14
15 **Abstract.**

16
17 While both surface water and groundwater hydrological systems exhibit structural, hydraulic
18 and chemical heterogeneity, and signatures of self-organisation, modelling approaches
19 between these two “water world” communities generally remain separate and distinct. To
20 begin to unify these water worlds, we recognize that preferential flows, in a general sense, are
21 a manifestation of self-organisation; they hinder perfect mixing within a system, due to a
22 more “energy efficient” and hence faster throughput of water and matter. We develop this
23 general notion by detailing the role of preferential flow for residence times and chemical
24 transport, as well as for energy conversions and energy dissipation associated with flows of
25 water and mass. Our principal focus is on the role of heterogeneity and preferential flow and
26 transport of water and chemical species. We propose, essentially, that related
27 conceptualizations and quantitative characterisations can be unified in terms of a theory that
28 connects these two water worlds in a dynamic framework. We discuss key features of fluid
29 flow and chemical transport dynamics in these two systems – surface water and groundwater
30 – and then focus on chemical transport, merging treatment of many of these dynamics in a
31 proposed quantitative framework. We then discuss aspects of a unified treatment of surface
32 water and groundwater systems in terms of energy and mass flows, and close with a reflection
33 on complementary manifestations of self-organisation in spatial patterns and temporal
34 dynamic behaviour.

35
36
37
38 **Keywords:** Chemical transport, Continuous Time Random Walk (CTRW), self-organisation,
39 preferential flow

44 1 INTRODUCTION

45 While surface and subsurface flow and transport of water and chemicals are strongly
46 interrelated, the catchment hydrology (“surface water”) and groundwater communities are
47 split into two “water worlds”. The communities even separate terminology, writing “surface
48 water” as two words but “groundwater” as one word!

49 At a very general level, it is well recognized that both catchment systems and groundwater
50 systems exhibit enormous structural and functional heterogeneity, which are, e.g., manifested
51 through the emergence of preferential flow and space-time distributions of water, chemicals,
52 sediments and colloids, and energy across all scales and within/across compartments (soil,
53 aquifers, surface rills and river networks, full catchment systems, and vegetation). Dooge
54 (1986) was among the first hydrologists who distinguished between different types of
55 heterogeneity – namely, between stochastic and organised/structured variability – and
56 reflected upon how these forms affect predictability of hydrological dynamics. He concluded
57 that most hydrological systems fall into Weinberg’s (1975) category of organised complexity
58 – meaning that they are too heterogeneous to allow pure deterministic handling but exhibit too
59 much organisation to enable pure statistical treatment.

60 A common way to define spatial organisation of a physical system is through its distance
61 from the maximum entropy state (Kondepudi and Prigogine, 1998; Kleidon, 2012). Isolated
62 systems, which do not exchange energy, mass, or entropy with their environment, evolve due
63 to the second law of thermodynamics to a perfectly mixed “dead state” called thermodynamic
64 equilibrium. In such cases, entropy is maximized and Gibbs free energy is minimized,
65 because all gradients have been dissipated by irreversible processes. Hydrological systems
66 are, however, open systems, as they exchange mass (water, chemicals, sediments, colloids),
67 energy and entropy across their system boundaries with their environment. Hydrological
68 systems may hence persist in a state far from thermodynamic equilibrium. They may even
69 evolve to states of a lower entropy, and thus stronger spatial organisation, for instance through
70 steepening of gradients, for example, in topography, or in the emergence of structured
71 variability of system characteristics or network-like structures. Such a development is referred
72 to as “self-organisation” (Haken, 1983) because local scale dissipative interactions, which are
73 irreversible and produce entropy, lead to ordered states or dynamic behaviours at the (macro-)
74 scale of the entire system. Self-organisation requires free energy transfer into the system to
75 perform the necessary physical work, self-reinforcement through a positive feedback to assure
76 “growth” of the organised structure/patterns in space, and the export of the entropy which is
77 produced within the local interactions to the environment (Kleidon, 2012).

78 Manifestations of self-organisation in *catchment systems* are manifold. The most obvious
79 one is the persistence of smooth topographic gradients (Reinhardt and Ellis, 2015; Kleidon et
80 al. 2012), which reflect the interplay of tectonic uplift and the amount of work water and biota
81 have performed to weather and erode solid materials, to form soils and create flow paths.
82 Although these processes are dissipative and produce entropy, they nevertheless leave
83 signatures of self-organisation in catchment systems. These are expressed, for instance,
84 through the soil catena – a largely deterministic arrangement of soil types along the
85 topographic gradient of hillslopes (Milne, 1931; Zehe et al., 2014) – and even more strongly
86 through the formation of rill and river networks (Fig. 1) at the hillslope and catchment scales

87 (Howard, 1990; Paik and Kumar, 2010; Kleidon et al., 2013). These networks form because
88 flow in rills is, in comparison to sheet flow, associated with a larger hydraulic radius, which
89 implies less frictional energy dissipation per unit volume of flow. This causes higher flow
90 rates, which in turn may erode more sediment. As a result, these networks commonly increase
91 the efficiency in transporting water, chemicals, sediments and energy through hydrological
92 systems, which results also in increased kinetic energy transport through the network and
93 across system boundaries.

94 In contrast, the term self-organisation is rarely applied to *groundwater systems*, except in
95 the context of positive/negative feedbacks during processes of precipitation and dissolution
96 (e.g., Worthington and Ford, 2009). We argue, though, that the subsurface, too, displays some
97 characteristics of (partial) self-organisation. This is manifested, in particular, through
98 ubiquitous, spatially correlated, anisotropic patterns of aquifer structural and hydraulic
99 properties, particularly in non-Gaussian systems (Bardossy, 2006), as these have much
100 smaller entropy compared to spatially uncorrelated patterns. The emergence and persistence
101 of preferential pathways even in homogeneous sand packs (e.g., Hoffman et al., 1996; Oswald
102 et al., 1997; Levy and Berkowitz, 2003) is a striking example of formation of a self-organised
103 pattern of “smooth fluid pressure gradients”.

104



105

106 **Figure 1** Hillslope scale rill networks developed during an overland flow event at the
107 Dornbirner Ach Austria (left panel, we gratefully acknowledge the Copyright holder © Ulrike
108 Scherer KIT) and the South Fork of Walker Creek in California (right panel, we gratefully
109 acknowledge the Copyright holder © James Kirchner ETH Zürich)

110

111 Our general recognition is that hydrological systems exhibit – below and above ground –
112 both (structural, hydraulic and chemical) heterogeneity and signatures of (self-)organisation.
113 We propose that all kinds of preferential flow paths/flow networks veining the land surface
114 and the subsurface are prime examples of spatial organisation (Bejan et al., 2008; Rodriguez-
115 Iturbe and Rinaldo, 2001) because they exhibit, independently of their genesis, similar
116 topological characteristics. Our starting point to unify both water worlds is the recognition
117 that any form of preferential flow is a manifestation of self-organisation, because it hinders
118 perfect mixing within a system and implies a more “energy efficient” and hence faster
119 throughput of water and matter (Rodriguez-Iturbe et al., 1999; Zehe et al., 2010; Kleidon et
120 al., 2013). This general notion can be elaborated further by detailing the role of preferential
121 flow for transport of mass and chemical species, and related fingerprints in travel distances or

122 travel times, as well as for energy conversion and energy dissipation associated with flows of
123 water.

124 In terms models, hydrological modelling (and hydrological theory) attempts to predict
125 how processes described by equations evolve in and interact with a structured heterogeneous
126 domain (i.e., hydrological landscape). However, our key argument that both systems are
127 subject to similar manifestations of self-organisation does not imply proposed use of a single
128 model. Rather, we argue that similar conceptualisations and methods of quantification –
129 whether related to preferential flow paths, dynamics and patterning of chemical transport and
130 reactivity, or characterization in terms of energy dissipation and entropy production, for
131 example – can and should be applied to both catchment and groundwater systems, to the
132 benefit of both research communities. The main focus of this contribution is on the role of
133 heterogeneity and preferential flow and transport of water and chemical species. At a general
134 level, we show that preferential flow causes deviations from the maximum entropy state,
135 though these deviations have different manifestations depending on whether we observe
136 solute transport in space or in time. Based on this insight, we propose, essentially, that related
137 conceptualisations and quantitative characterisations can be unified in terms of a theory that is
138 applicable in catchment and groundwater systems, and thus connects these two “water
139 worlds”.

140 We first discuss key features of fluid flow and chemical transport dynamics in these two
141 systems – catchments (including surface water) and groundwater – using the (often distinct)
142 terminology of each of these “water world” research communities. We outline the particular
143 questions, methods, limitations, and uncertainties in each “world” (Section 2). We then focus
144 on chemical transport, merging treatment of many of these dynamics in a proposed
145 quantitative framework, and providing specific examples (Section 3). More specifically,
146 Section 3 first defines specific conceptual and quantitative tools, and within this context,
147 introduces a continuous time random walk (CTRW) modelling framework with a clear
148 connection to microscale physics and to the well-known advection-dispersion equation.
149 Section 3 then offers new insights, in terms of contrasting power law and inverse gamma
150 distributions – used in the groundwater literature to describe different travel time distributions
151 that control long tailing in breakthrough curves – to gamma distributions used more often in
152 the surface water (catchment system) literature. This analysis is a basis for suggesting how
153 surface water systems (catchment response to chemical transport) can be treated within the
154 CTRW framework. Final conclusions and perspectives appear in Section 4. Throughout, we
155 attempt to offer an innovative synthesis of concepts and methods from the generally disparate
156 surface water (catchment hydrology) and groundwater research communities. Each
157 community has developed sophisticated modelling and measurement capabilities – which
158 have led to significant scientific advances over the last two decades – that could benefit the
159 other community and help address outstanding, unsolved problems.

160 Before proceeding, we emphasise that our use of the term “two water worlds” throughout
161 this paper is intended to highlight the disparate catchment and groundwater communities, and
162 is not used in the specific context of mobile-immobile water in the root zone (McDonnell,
163 2014), as discussed at the end of Section 3.1.

164 2 TWO WATER WORLDS – UNIQUE, DIFFERENT AND SIMILAR

165 2.1 Governing laws of fluid flow, the momentum balance and energy 166 dissipation

167 In both water worlds, a major focus is on travel distances, as well as travel times
168 (residence times) of water, as they provide the main link between water quantity and quality
169 (Hrachowitz et al., 2016). Catchment hydrology deals also with extremes, i.e., floods and
170 droughts, as well as land surface-atmosphere feedbacks, fluvial geomorphology and eco-
171 hydrology.

172 From the outset, we recognise that predictions of water dynamics in catchment and aquifer
173 systems require joint treatment of their mass, momentum and energy balances. Catchment
174 science and modelling has, traditionally, a strong focus on catchment mass and (in part)
175 energy balances, as evaporation and transpiration release energy in the form of latent heat to
176 the atmosphere. The momentum balance is treated in an implicit conceptualised manner, as
177 detailed below. Predictions of fluid flow in groundwater systems rely on the joint treatment of
178 the mass and the stationary momentum balances using Darcy’s law, while the energy balance
179 appears at first sight of low importance.

180 Chemical transport and travel times through hydrological systems are, however, strongly
181 related to both the momentum and the energy balances, because they jointly control the
182 spectrum of fluid velocities and the direction of streamlines. The governing equations that
183 characterise water flow velocities along the land surface and in groundwater systems are
184 simplifications of the Navier-Stokes equations (Eq. 1), which describe the momentum balance
185 of the fluid as an interplay of driving forces and hindering frictional forces:

$$186 \quad \rho \frac{\partial \mathbf{v}}{\partial t} + (\mathbf{v} \cdot \nabla) \mathbf{v} = -\nabla p - \rho \mathbf{g} + \eta \Delta^2 \mathbf{v} \quad (\text{Eq. 1})$$

187 where \mathbf{v} (m s⁻¹) is the fluid velocity vector, \mathbf{g} (m s⁻²) the gravitation acceleration vector, ρ (kg
188 m⁻³) the water density, and η the dynamic viscosity (kg m⁻¹ s⁻¹) of the fluid.

189 2.1.1 Surface water flow and Manning’s law

190 Overland and channel flow are driven by surface topography, or more precisely, by
191 gravitational potential energy differences, but only minute amounts of these energy
192 differences are converted into kinetic energy of the flow (Loritz et al., 2019), while the rest is
193 dissipated. Surface water flow velocity is often characterised by Manning’s law (Eq. 2), a
194 steady-state, one-dimensional approximation of the Navier-Stokes equation that neglects
195 inertial acceleration for the case of turbulent shear stress and thus turbulent energy
196 dissipation. Fluid velocity grows proportional to the square root of the driving hydraulic head
197 gradient; the latter corresponds to the potential energy of a unit mass of water:

$$198 \quad \mathbf{v}_{\text{surface}} = -\frac{R^{\frac{2}{3}}}{n} \sqrt{2g \nabla_{x,y} (h + z)} = -\frac{R^{\frac{2}{3}}}{n} \sqrt{2g \nabla_{x,y} \Phi_H} \quad (\text{Eq. 2})$$

199 where $\mathbf{v}_{\text{surface}}$ (m s⁻¹) is the overland flow velocity vector, R (m) the hydraulic radius defined
200 as the ratio of the wetted cross-section A_{wet} (m²) to the wetted perimeter U_{wet} (m), n is
201 Manning’s roughness (m^{-1/3}), z (m) is topographical elevation, h (m) is depth of the flow, and
202 Φ (m) is the total hydraulic head.

203 Moreover, as friction occurs mainly at the contact line between the fluid and the solid, the
204 hydraulic radius R (m) can be used to scale the ratio between driving gravity force and the

205 hindering frictional dissipative force. Kleidon et al. (2013) classified this as a “weak form” of
 206 dissipative interaction between fluid and solid. In this context, they showed that overland flow
 207 in rills implies, due to the larger hydraulic radius, a smaller dissipative loss per unit volume
 208 and thus a higher energy efficiency compared to sheet flow. Along the same line, they showed
 209 that flow in a smaller number of wider channels is more efficient than flow in a higher
 210 number of narrower channels. Both effects, flow in rills and channelling, lead to a higher fluid
 211 velocity, and thus a higher power (kinetic energy) flux through the network. Note that a 10%
 212 faster fluid velocity implies 30% more power as the latter grows with the cube of the fluid
 213 velocity.

214 **2.1.2 Subsurface flow and Darcy’s law**

215 Flow through subsurface porous media, on the other hand, is driven by the gradient in
 216 total hydraulic head, reflecting differences in gravitational potential, matric potential and
 217 pressure potential energies as described in the respective forms of Darcy’s law (Eq. 3). The
 218 latter is also a steady state, one dimensional approximation of the Navier-Stokes equation
 219 neglecting the inertial terms. However, in this case flow is essentially laminar and dissipative
 220 frictional losses in the porous medium are so much larger than in open surface flow, that
 221 kinetic energy can be neglected. When solving the Darcy law (Eq. 3, first line) for the
 222 interstitial travel velocities and defining the flow resistance as inverse hydraulic conductivity,
 223 one obtains a form of the Darcy law (Eq. 3, second line) which is similar to Manning’s law
 224 (Eq. 2). The main difference arises from the different dependencies on the hydraulic head
 225 gradient, reflecting the turbulent and laminar flow regimes, respectively:

$$\begin{aligned}
 227 \quad \mathbf{q}_{vadose} &= -k(\theta)\nabla(\psi + z), \quad \mathbf{q}_{gw} = -k_s\nabla(H + z) \\
 228 \quad \mathbf{v}_{vadose} &= -\frac{1}{\theta R(\theta)}\nabla\Phi_{vadose}, \quad \mathbf{v}_{gw} = -\frac{1}{\theta_s R_s}\nabla\Phi_{gw} \text{ (Eq. 3)} \\
 229 \quad R(\theta) &= 1/k(\theta), R = 1/k_s, \Phi_{vadose} = (\psi + z), \Phi_{gw} = (H + z)
 \end{aligned}$$

230
 231 where \mathbf{q}_{vadose} and \mathbf{q}_{gw} (m s^{-1}) are water flux vectors (filter velocities) in the partially saturated
 232 and saturated zones, respectively, \mathbf{v}_{vadose} and \mathbf{v}_{gw} (m s^{-1}) are the respective interstitial travel
 233 velocities, θ and θ_s are the soil water content (-) and the porosity (-), $k(\theta)$ and k_s (m s^{-1}) are the
 234 partially saturated and saturated hydraulic conductivity, ψ (m) and H (m) denote the capillary
 235 pressure and pressure potentials, and Φ_{vadose} and Φ_{gw} are total hydraulic heads in the partially
 236 saturated and saturated zones.

237 The strikingly high dissipative nature of porous media flow becomes obvious when
 238 recalling that the driving matric potential gradients in the vadose zone are often orders of
 239 magnitude larger than 1 m m^{-1} . This implies a capillary acceleration term much larger than
 240 Earth’s gravitational acceleration g (m s^{-2}), yet fluid velocities in the porous matrix are several
 241 orders of magnitude smaller than in surface water systems. However, the generally much
 242 slower fluid velocity in groundwater systems does not impose a slow hydraulic response time
 243 during rainstorms; on the contrary, aquifers may release – almost instantaneously – “older”,
 244 pre-event water into a catchment outlet stream. This apparent paradox – referred to often as
 245 the “old-new water paradox” (Kirchner, 2003) – is explained by propagation of pressure
 246 waves. Shear or compression waves (or waves in general) transport momentum and energy

247 through continua *without an associated transport of mass or particles* (Everett, 2013;
248 Goldstein, 2013); and group velocity (or “celerity”) is many orders of magnitude larger than
249 the fluid velocity in aquifer systems (McDonnell and Beven, 2014). Today, it is known that
250 depending on landscape setting, antecedent wetness conditions, and the dominant runoff
251 mechanisms, pre-event water fractions in storm runoff can vary from near zero to more than
252 60% of storm water having an isotopic signature different from that of rainfall (Sklash and
253 Farvolden, 1979; Sklash et al., 1996; Blume et al., 2008).

254 **2.1.3 Preferred flow paths as maximum power structures and non-Fickian** 255 **transport**

256 Flow velocity within subsurface preferential pathways (macropores, pipes, fractures) is
257 known to be much faster than matrix flow (Beven and Germann, 1982, 2013). This is caused
258 not only by the vanishing capillary forces, but also, largely, by the strong reduction in
259 frictional dissipation in macropores compared to flow in the porous matrix. Viscous
260 dissipation in preferential pathways occurs, similar to open channel flow, mainly at the
261 contact line between fluid and solid, i.e., the wetted perimeter of the macropore, which
262 implies – similar to the case of rill and river networks – a larger hydraulic radius and thus a
263 much more energy efficient flow (Zehe et al., 2010). Darcy’s law is hence inappropriate to
264 characterise preferential flow (Germann, 2018). Clearly, rapid localised flow and transport in
265 preferential pathways hinders the transition from imperfectly mixed stochastic advective
266 transport in the near field to well mixed advective dispersive transport in the far field.
267 Predictions of solute plumes and travel times in the near field are thus challenging as this
268 requires detailed knowledge of the velocity field, while transport at the well-mixed Fickian
269 limit depends on the average fluid velocity and the dispersion coefficient (Simmons, 1982;
270 Sposito et al., 1986; Bodin, 2015).

271 Although the revisited laws, interactions and phenomena are well known, we suggest that
272 the energy point of view yields a unifying perspective to explain why macropore, rill and river
273 networks are the preferred (preferential) pathways for water flow on land and below. One
274 might hence expect that water flows along the path of maximum power (Howard, 1990;
275 Kleidon, 2013), which is the product of the flow velocity times the driving potential
276 difference. The paths of maximum power correspond in the case of constant friction to the
277 path of steepest descent in hydraulic head, while in the case of a constant gradient, it
278 corresponds to the path of minimum flow resistance (Zehe et al., 2010). From the discussion
279 above, we further conclude that catchment hydrology and groundwater hydrology are
280 inseparable. We can neither separate a river from its catchment and its subsurface, nor an
281 aquifer from the land surface and the catchment. Both stream flow response to rainfall and
282 groundwater are composed of “waters of different ages”, reflecting the ranges of overland
283 flow, subsurface storm flow and base-flow contributions with their specific velocities, usually
284 non-Fickian travel time distributions, and chemical signatures.

285 In the following, we elaborate briefly on the specific model paradigms in catchment and
286 groundwater hydrology with an emphasis on preferential pathways for fluid flow and
287 chemical transport, and on the resulting ubiquitous, anomalous early and late time arrivals of
288 chemicals to measurement outlets.

289 **2.2 Catchment hydrology from the water balance to solute transport**

290 **2.2.1 The catchment concept and the duality in water balance modelling**

291 Catchment hydrology developed largely as an engineering discipline around traditional
292 tasks of designing and operating reservoirs, flood risk assessment and water resources
293 management (Sivapalan, 2018). Although the catchment concept is elementary to these tasks,
294 we think it worthwhile to reflect briefly on it here. The watershed boundary delimits a control
295 volume where the streamlines are expected to converge into the river network, hence ideally,
296 the entire set of surface and subsurface runoff components feeds the stream. We can thus
297 characterise the water balance of an ideally closed catchment control volume based on
298 observations of rainfall input and stream flow response (with uncertainty). Even more
299 importantly, the catchment water balance can be solved without an explicit treatment of the
300 momentum balance, because flow lines end up in the stream.

301 This is a twofold blessing. First, hydrological models can be benchmarked against integral
302 water balance observations. We posit that this unique property of catchments is *the* reason
303 why integral conceptual hydrological models, which largely ignore the momentum balance,
304 allow successful predictions of stream flow the catchment outlet (Sivapalan, 2018). As
305 conceptual models directly address processes at the system level without accounting for
306 subscale mechanistic reasons, their application is often referred to as “top down” modelling.
307 The other end of the model spectrum consists of physics-based, spatially distributed models,
308 originally proposed by the blueprint of Freeze and Harlan (1969), which follow a “bottom up”
309 mechanistic paradigm. These models are thus also referred to as reductionist models. While
310 the pros and cons of top down conceptual models and bottom up physics-based models have
311 been discussed extensively, we agree with Hrachowitz and Clark (2017) that they offer
312 complementary merits as detailed below. As an aside, it is interesting to reflect why
313 conceptual models do not exist in the field of, e.g., meteorology. We suggest that this is
314 because atmospheric flows are not governed by mechanisms similar to catchments, which
315 implies that the amount of air mass flowing from one location to another cannot be predicted
316 without knowing the flow lines.

317 **2.2.2 Top down modelling of the catchment water balance**

318 Top down conceptual hydrological models simulated water storage, redistribution and
319 release within the catchment system through combination of non-linear and linear reservoirs,
320 characterised by effective state variable and effective parameters and effective fluxes
321 (Savenije and Hrachowitz, 2017). Due to their mathematical simplicity, conceptual models
322 are straightforward to code. With the advent of combinatorial optimization methods for
323 automated parameter search, and fast computers (Duan et al., 1992; Bardossy and Singh,
324 2008; Vrugt and Ter Braak, 2011), these models became, at first sight, also straightforward to
325 apply. Automated, random parameter search led, however, to the discovery of the well-known
326 equifinality problem – namely, that several model structures or parameter sets may reproduce
327 the target data in an acceptable manner (Beven and Binley, 1992), within the calibration and
328 validation period, but these models and parameter sets yield uncertain future predictions (e.g.,
329 Wagener et al., 2006). Equifinality and related parameter uncertainty arises from the ill-posed
330 nature of inverse parameter estimation and from parameter interactions in the equations.
331 While the first problem can be tackled using multi-objective and multiresponse calibration (e.g.,

332 Mertens et al., 2004; Ebel and Logue, 2006; Fenicia et al., 2007), the latter is inherent to the
333 model equations regardless of whether they are conceptual (as shown by Bardossy (2007) for
334 the Nash cascade), or physically based (as shown by, e.g., Klaus and Zehe (2010) and Zehe et
335 al. (2014)).

336 A well-known shortcoming of conceptual models is that their key parameters cannot be
337 measured directly. This motivated numerous parameter regionalization efforts (He et al.,
338 2011a) to relate conceptual parameters to measurable catchment characteristics, typically
339 broadly available data on soils (including texture), land use, and topography. As a
340 consequence, such functions have been derived successfully, for example, to relate parameters
341 of the soil moisture accounting scheme to soil type and land use (as shown by, e.g., Hundecha
342 and Bardossy, 2004; Samaniego and Bardossy, 2006; He et al., 2011b; Singh et al., 2016) or
343 parameters of the soil moisture accounting of the mHm (Samaniego et al., 2010) to soil
344 textural data. As such, relations are landscape-specific and they require a new calibration
345 when moving to new target areas. This is of course possible if high quality discharge data are
346 available. Yet, due to the incompatibility between the corresponding measurement and
347 observations scales, these regionalisation functions are not straightforwardly explained using
348 physical reasoning. This is true even if soil moisture accounting from soil physics is used,
349 e.g., the Brooks and Corey (1964) soil water retention curve, as in the case of the mHm
350 model.

351 A number of early efforts to meaningfully define hydrological response units for regional
352 modelling of hydrological landscapes were reported by, e.g. Knudsen et al. (1986), Flügel
353 (1995), and Winter (2001). Savenije (2010) and Fenicia et al. (2011) significantly improved
354 the link between conceptual models and landscape structure in their flexible model
355 framework. The key idea is to subdivide the landscape into different functional units
356 (plateaus, hillslopes, wetlands, rivers), and to represent each of them by a specific
357 combination of conceptual model components to mimic their dominant runoff generation
358 processes. Landscapes with different dominant runoff generation mechanisms are represented
359 through an appropriate combination of these conceptual “building blocks” (Fenicia et al.,
360 2014; Gao et al., 2014; Wrede et al., 2015) using suitable topographical signatures such as
361 “Height Above Next Drainage” (Gharari et al., 2011) to estimate their areal share. This is a
362 clear advantage that facilitates model calibration and reduction of predictive uncertainty.

363 The strength of integral conceptual models is their ability to provide parsimonious and
364 reliable predictions of streamflow Q ($\text{m}^3 \text{s}^{-1}$) directly at the catchment outlet. However, it is
365 nevertheless not straightforward to apply the models for predictions of transport of tracers,
366 and more generally chemical species through the catchment into a stream, as elaborated in the
367 following.

368 **2.2.3 Integral approaches to solute transport modelling in catchment hydrology**

369 Predictions of solute transport require information about the spectrum of fluid velocities
370 and travel distances across the various flow paths into the stream (we can usually neglect the
371 travel time within the river network due to the much higher fluid velocities, as argued in Sect.
372 3.1). Such information can generally be inferred from breakthrough curves of tracers that
373 enter and leave the system through well-defined boundaries, as shown for instance by the
374 early work of Simmons (1982) and Jury et al. (1986), using transfer functions to model solute

375 transport through soil columns. The transfer function approach is based on the theory of linear
376 systems. This implies that the outflow concentration (volumetric flux-averaged concentration)
377 C_{out} (kg m^{-3}) at time t is, in case of steady-state water flow, the convolution of the solute
378 input time series C_{in} with the system function G (Green's function):
379

$$380 \quad C_{out}(t) = \int_0^{\infty} G(t - \tau) C_{out}(\tau) d\tau \quad (\text{Eq. 4})$$

381
382 The transfer function is the system response to a delta function input. Note that Eq. 4
383 should in general be formulated for the input and output mass flows, which correspond to the
384 input/output concentration multiplied by the input/output volumetric water flows. It is
385 important to note in this context is that the average travel time through the system can be
386 calculated from the water flow and length of flow path, as the average travel velocity
387 corresponds to the flow divided by the wetted cross section of the soil column (see Eq. 3). The
388 latter implies that travel time distributions through partially saturated soils are transient and
389 hence constrained by the input time (Jury et al., 1986; Sposito et al. 1986). The well-known
390 fact that the flow velocity field changes continuously with changing soil water content
391 explains why transfer function approaches have been largely put aside in soil physics and
392 solute transport modelling in the partially saturated zone.

393 In the case of catchments, simulated runoff from conceptual hydrological models cannot,
394 unfortunately, be used to constrain the average transport velocity. This is simply because
395 conceptual models provide, by definition, no information about the wetted cross of the flow
396 path through the catchment, and the latter determines essentially the average fluid velocity v
397 from simulated total runoff Q . The fact that the simple equation $Q = v_{transport} A_{wet}$ has an
398 infinite solution space, if A_{wet} is unknown, is also a major source of equifinality. This was
399 shown by Klaus and Zehe (2010) and Wienhöfer and Zehe (2014), using a physically-based
400 hydrological model to investigate the role of vertical lateral preferential flow paths of
401 hillslope rainfall runoff response. These authors found that several network configurations
402 matched the observed flow response equally well: some configurations consisted of a small
403 number of larger macropores of higher conductance, while others consisted of a higher
404 number of less conductive macropores. Overall, these configurations yielded the same
405 volumetric water flow, but they performed rather differently with respect to simulation of
406 solute transport. An even larger challenge for transport modelling through catchments arises
407 from the fact that the distribution of flow path lengths is even more difficult to constrain,
408 compared to a soil column.

409 Despite these challenges, the tracer hydrology community made considerable progress in
410 understanding catchment transit time distributions and predicting isotope or tracer
411 concentrations in streamflow (Harman, 2015). Initially, stable isotopologues of the water
412 molecule and other tracers gained attention as they allow a separation of the storm hydrograph
413 into pre-event and event water fractions using stable end member mixing (Bonell et al., 1990;
414 Sklash et al., 1996). Today isotopes of the water molecules and water chemistry data are used
415 as a continuous source of information to infer travel time distributions of water through
416 catchments (McGlynn et al., 2002; McGlynn and Seibert, 2003; Weiler et al., 2003; Klaus et
417 al., 2013). Early attempts to predict tracer concentrations in the stream relied on the same kind
418 of transfer functions as outlined in Eq. (4) for soil columns. Hence, they naturally faced the

419 same problems of state and thus time-dependent travel time distributions (Hrachowitz et al.,
420 2013; Klaus et al., 2015; Rodriguez et al., 2018). More recent approaches rely on age ranked
421 storage as a “state” variable in combination with StoreAgeSelection (SAS) functions for
422 stream flow and evapotranspiration to infer their respective travel time distributions (Harmann
423 et al. 2015; Rinaldo et al., 2015). Aged ranked storage needs to be inferred from solving the
424 Master equation, i.e., the catchment water balance for each time and each age. This can be
425 done either by using conceptually modelled or observed discharge and evapo-transpiration,
426 and it requires a proper selection of the functional form of the SAS functions and optionally
427 their time-dependent weights (Rodriguez and Klaus, 2019). Related studies rely on a single or
428 several gamma distributions (Hrachowitz et al., 2010; Klaus et al., 2015; Rodriguez and
429 Klaus, 2019), others used the beta distribution (van der Velde et al., 2012) or piece-wise linear
430 distributions (Hrachowitz et al., 2013, 2015).

431 Here we propose that the continuous time random walk (CTRW) framework from the
432 groundwater “world” has much to offer to catchment travel time modelling (as detailed in
433 Sect. 3). We show that, in particular, the inverse gamma distribution may offer a useful
434 alternative that offers the asset of a clear connection to microscale physics and the well-
435 known advection-dispersion equation, which is used in bottom up modelling (Sect. 2.2.4). In
436 this context, it is interesting to recall that catchments were modelled as time-invariant linear
437 systems for a considerable time, since the unit hydrograph was introduced by Sherman
438 (1932). While the effect of precipitation was calculated using runoff coefficients, the
439 streamflow response was simulated by convoluting effective precipitation with the system
440 function, i.e., the unit hydrograph. The “Nash” cascade of linear reservoirs was a popular
441 means to describe the unit hydrograph in a parametric form, and it is well known that the
442 latter is mathematically equivalent to a gamma distribution (Nash, 1957). As streamflow
443 response of the catchment is affected largely by surface and subsurface preferential pathways,
444 which cause non-Fickian transport, one might hence wonder whether a gamma distribution
445 function is an ideal choice to represent the fingerprint of preferential flow.

446 **2.2.4 Bottom up modelling of the catchment water balance**

447 The blueprint of a physically based hydrological, introduced by Freeze and Harlan (1969),
448 has found manifold implementations. Physically-based models like MikeShe (Refsgaard and
449 Storm, 1995) or CATHY (Camporese et al., 2010) typically rely on the Darcy-Richards
450 concept for soil water dynamics (Eq. 3), the Penman–Monteith equation for soil-vegetation-
451 atmosphere exchange processes, and the Manning’s equation for estimating overland and
452 stream flow velocities (Eq. 2).

453 Each of these approaches is naturally subject to limitations, reflecting our yet imperfect
454 understanding, and suffers from the limited transferability of their related parameters from
455 idealised, homogeneous laboratory conditions to heterogeneous and spatially organised
456 natural systems (Grayson et al., 1992; Gupta et al., 2012). In this context, the Darcy-Richards
457 model receives by far the strongest criticism (Beven and Germann, 2013), simply because the
458 underlying assumption regarding the dominance of capillarity-controlled diffusive flow, under
459 local equilibrium conditions, is largely inappropriate when accounting for preferential flow.
460 The Darcy model is hence incomplete when accounting for infiltration (Germann, 2018) and
461 preferential flow, and several approaches have been proposed to close this gap. These range

462 from the early idea of (a) stochastic convection assuming no mixing at all (Simmons, 1982),
463 to (b) dual-permeability conceptualizations relying on overlapping, exchanging continua
464 (Šimunek et al., 2003), to (c) spatially explicit representations of macropores as connected
465 flow paths (Vogel et al., 2006; Sander and Gerke, 2009; Zehe et al., 2010; Wienhoefer and
466 Zehe, 2014; Loritz et al., 2017), and to (d) pore-network models based on mathematical
467 morphology (Vogel and Roth, 2001). An alternative approach to dealing with preferential
468 flow and transport employs Lagrangian models such as SAMP (Ewen, 1996a,b), MIPs
469 (Davies and Beven, 2012; Davies et al., 2013), and LAST (Zehe and Jackisch, 2016; Jackisch
470 and Zehe, 2018; Sternagel et al., 2019).

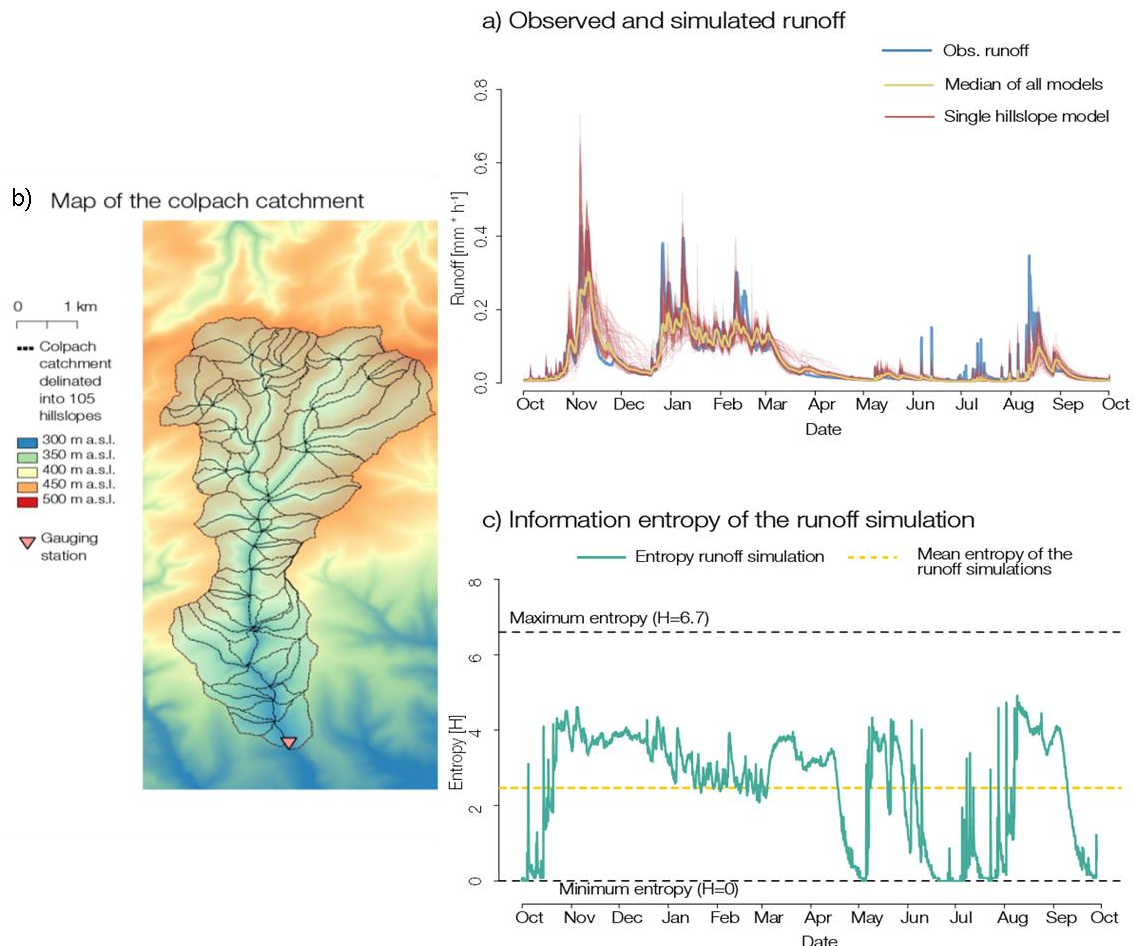
471 Reductionist models are, despite the challenge to represent preferential flow and transport,
472 indispensable tools for scientific learning. They particularly allow exploration of how
473 distributed patterns and their spatial organisation jointly controls distributed state dynamics
474 and integral behaviour of hydrological systems (Zehe and Blöschl, 2004). Related studies
475 range from, e.g., the investigation of (a) how changes in agricultural practices affect the
476 stream flow generation in a catchment (Pérez et al., 2011), (b) the role of bedrock topography
477 for runoff generation using (Hopp and McDonnell; 2009) at the Panola hillslope and the
478 Colpach catchment (Loritz et al. 2017), or (c) the role of vertical and lateral preferential flow
479 networks on subsurface water flow and solute transport at the hillslope scale (Bishop et al.,
480 2015; Wienhöfer and Zehe; 2014; Klaus and Zehe; 2011; Klaus and Zehe, 2010), including
481 the issue of equifinality. Setting up a physically-based model, however, requires an enormous
482 amount of highly resolved spatial data, particularly on subsurface characteristics. Such data
483 sets are rare, and the “hunger” for data in such models risks a much higher structural model
484 uncertainty. On the other hand, these models offer also greater opportunities for constraining
485 their structure using multiple data orthogonal to discharge (Ebel and Logue, 2006; Wienhöfer
486 and Zehe, 2014).

487 Another asset of reductionist models is their thermodynamic consistency, which implies
488 that energy conversions related to flow and storage dynamics of water in the catchment
489 systems are straightforward to calculate (Zehe et al, 2014). This offers the opportunity to test
490 the feasibility of thermodynamic optimality as constraint for parameter inference (Zehe et al.;
491 2013), the latter is rather challenging when using conceptual (Westhoff et al., 2013, Westhoff
492 et al., 2016). More recent applications demonstrated, in line with this asset, new ways to
493 simply distributed models without lumping, which allowed the successful simulation of the
494 water balance of a 19 km² large catchment using a single effective hillslope model (Loritz et
495 al., 2017). The key to this was to respect energy conservation during the aggregation
496 procedure, specifically through derivation of an effective topography that conserved the
497 average distribution of potential energy along the average flow path length to the stream; and
498 through a macroscale effective soil water retention curve that conserved the relation between
499 the average soil water content and matric potential energy using a set point scale retention
500 experiments (Jackisch 2015; Zehe et al., 2019).

501 Along similar lines, Loritz et al. (2018) showed that simulations using a fully distributed
502 setup of the same Colpach catchment using 105 different hillslopes yielded strongly
503 redundant contributions of stream flow (Fig. 2). They used the Shannon entropy (Shannon,
504 1948, defined in Eq. 6 in section 2.4) to quantify the diversity in simulated runoff of the
505 hillslope ensemble at each time step. They found that although the entropy of the ensemble

506 was rather dynamic in time, it never reached the maximum value. Note that an entropy
 507 maximum implies that hillslopes contribute in a unique fashion, while a value of zero implies
 508 that all hillslope yield a similar runoff response. They further showed that the fully distributed
 509 model, consisting of 105 hillslopes, can be compressed to a model using 6 hillslopes with
 510 distinctly different runoff responses, without a loss in simulation performance. Based on these
 511 findings, they concluded that spatial organisation leads to emergence of functional similarity
 512 at the hillslope scale, as proposed by Zehe et al. (2014). This in turn explains why conceptual
 513 models can be reasonably applied as most of the spatial heterogeneity in the catchment seems
 514 to be irrelevant for runoff production. However, this is not the case, when it comes to
 515 transport of chemicals as elaborated in the next section.

516 In accord with Hrachowitz and Clark (2017), we conclude that top down and bottom up
 517 models indeed have complementary merits. Moreover, we propose that the applicability of
 518 conceptual models at larger scales arises from the fact that spatial organisation leads in
 519 conjunction with the strongly dissipative nature of hydrological process to the emergence of
 520 simplicity at larger scales (Savenije and Hrachowitz, 2017; Loritz et al., 2018).
 521



522
 523 **Figure 2** (a) Observed and simulated runoff of the Colpach catchment. The red lines
 524 correspond to individual hillslope models and the yellow line to area weighted median of all
 525 hillslopes. (b) Map of the Colpach catchment and the 105 different hillslopes. (c) Shannon
 526 entropy in turquoise for the runoff simulations as well as the corresponding mean. © Ralf
 527 Loritz KIT, from Loritz et al. (2018).

528 **2.3 Distributed solute transport modelling – the key role of the critical zone**

529 Reductionist physically models are straightforwardly to couple with the advection-
530 dispersion equation (compare Eq. 11 in Sect. 3) or particle tracking schemes to simulate
531 transport of tracers and reactive compounds through the critical zone into groundwater or
532 along the surface and through the subsurface into the stream.

533 The soil-vegetation-atmosphere-transfer system (SVAT-system), or in more recent terms,
534 the “critical” zone, is the mediator between the atmosphere and the two water worlds. This
535 tiny compartment controls the splitting of rainfall into overland flow and infiltration, and the
536 interplay among soil water storage, root water uptake and groundwater recharge. Soil water
537 and soil air contents control CO₂ emissions of forest soils, denitrification and related trace gas
538 emissions into the atmosphere (Koehler et al. 2010; Koehler et al, 2012), as well as
539 biogeochemical transformations of chemical species.

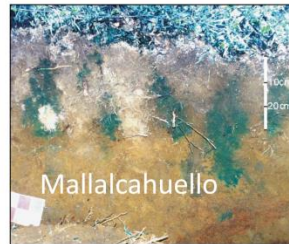
540 Partly saturated soils may, depending on initial their state and structure, respond with
541 preferential flow and transport of contaminants and nutrients through the biological most
542 active topsoil buffer (Flury et al., 1994, 1995; Flury, 1996; McGrath et al., 2008, 2010; Klaus
543 et al., 2014). Rapid transport operates within strongly localized preferential pathways such as
544 root channels, cracks, worm burrows or within connected inter-aggregate pore networks
545 which “bypass” of the soil matrix continuum (e.g., Beven and Germann, 1982; Blume et al.,
546 2009; Wienhöfer et al., 2009; Beven and Germann, 2013). The well-known fingerprint of
547 preferential flow is a “fingered” flow pattern, which is often visualised through dye staining
548 or two-dimensional concentration patterns in vertical soil profiles (Fig. 3). These reveal
549 imperfectly mixed conditions in the near field, which implies that the spatial concentration
550 pattern deviates from the well mixed Fickian limit over a relatively long time. The latter
551 corresponds in the case of a delta input to a Gaussian distribution of travel distances at a fixed
552 time, where the centre of mass travels with the average transport velocity while the spreading
553 of the concentration grows linearly with time proportional to the macrodispersion coefficient
554 (Simmons, 1982; Bodin, 2015). Note that according to Trefry et al. (2003), this Gaussian
555 travel distance corresponds to a state of maximum entropy. Preferential flow hence implies a
556 deviation from this well mixed maximum entropy state, which cannot be predicted with the
557 advection-dispersion equation (e.g., Roth and Hammel, 1996). A recent study (Sternagel et
558 al., 2019) revealed that even double domain models such as Hydrus 1D may fail to match the
559 flow fingers and/or long-time concentration tails in tracer profiles. Frequently, the partially
560 saturated region of the subsurface is simply too thin to allow perfectly mixed Gaussian travel
561 distances to be established; hence non-Fickian transport in the critical zone is today regarded
562 as being the rule rather than the exception.

563

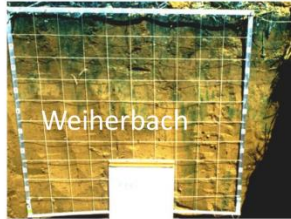
Germany, van Schaik et al. (2014)



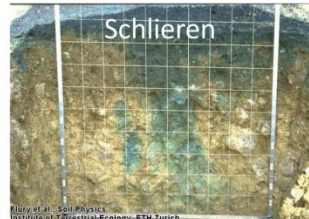
Chile, Blume et al. (2009) Austria, Wienhöfer et al. (2009)



Germany, Zehe and Flüher (2001)



Switzerland, Flury et al. (1994)



564
565
566
567
568
569
570
571
572

Figure 3 Finger flow pattern revealed from standardized dye staining experiments for a transport time of 1 day; images were generously provided by Flury et al. (2004; 2005; Copyright © 1994, 1995 the American Geophysical Union) for Switzerland, Blume et al. (2009, Copyright © Theresa Blume) for Chile, Wienhöfer et al. (2009, Copyright © Jan Wienhöfer KIT) for Austria, and Zehe and Flüher (2001, Copyright © Erwin Zehe KIT) and van Schaik et al. (2014, Copyright © 2013 John Wiley & Sons, Ltd.) for the German Weierbach.

573 Because preferential transport leads to strongly localized accumulation of water and
574 chemical species, preferential pathways are potential biogeochemical hotspots. This is
575 particularly the case for biopores such as worm burrows and root channels. Worm burrows
576 provide a high amount of organic carbon and worms “catalyse” microbiological activity due
577 to their enzymatic activity (Bundt et al., 2001; Binet et al., 2006; Bolduan and Zehe, 2006;
578 van Schaik et al., 2014). Similarly, plant roots provide litter and exude carbon substrates to
579 facilitate nutrient uptake. Intense runoff and preferential flow events optionally connect these
580 isolated “hot spots” to lateral subsurface flow paths such as a tile drain network or a pipe
581 network along the bedrock interface, and thereby establish “hydrological connectivity”
582 (Tromp-van Meerveld and McDonnell, 2006; Lehmann et al., 2007; Faulkner, 2008). The
583 onset of hydrological connectivity comprises again a “hot moment” as upslope areas and,
584 potentially, the entire catchment start “feeding” the stream with water, nutrients and
585 contaminants (Wilcke et al., 2001; Goller et al., 2006).

586 The critical zone, furthermore, crucially controls the Bowen ratio (the partitioning of net
587 radiation energy into sensible and latent heat), and soil water available to plants is a key
588 controlling factor. The residual soil water content is not available for plants, as it is generally
589 stored in fine pores subject to very high capillary forces. Isotopic tracers have been
590 fundamental to unravelling water flow paths in soils, using dual plots (Benettin et al., 2018;
591 Sprenger et al., 2018), and to distinguish soil water that is recycled to the atmosphere and
592 released as stream flow (Brooks et al., 2010; McDonnell, 2014).

593 Further to the above points, it is noted that laboratory and numerical studies of multiple
594 cycles of infiltration-drainage of water and chemicals into a porous medium demonstrate
595 clearly the establishment of stable “old” water clusters/pockets, and even a “memory effect”
596 (Kapetas et al., 2014), which remain even with multiple cycles of “new” water infiltration
597 (Gouet-Kaplan and Berkowitz, 2011). These pore-scale studies are in qualitative (and semi-
598 quantitative) agreement with studies at the *field scale*, which show similar retention behaviour
599 of bromide (introduced during the first infiltration cycle) after multiple infiltration-drainage
600 cycles (Turton et al., 1995; Collins et al., 2000). As a consequence, when each cycle of
601 infiltration contains water with a different chemical signature, stable pockets of water can be
602 established with highly varying chemical composition. We hence emphasise that mobile and
603 immobile waters sustaining evaporation and stream flow – and the chemical species they
604 contain – exist at a continuum of scales from the pore to the field level. Thus, rather than
605 attempting to delineate pockets of less and more mobile water at each scale – separating these
606 pockets at the pore, the column, the meter, the 10 meter, and the field and catchment scales –
607 we instead suggest recognising and delineating an “overall effect” of separation between
608 “old” (immobile) and “new” (mobile) waters at a given “effective” scale of interest, which
609 integrates over all such old and new waters. As we discuss in detail at the end of Sect. 3.1, and
610 thereafter, then, we argue that it is a more effective approach to consider chemical transport as
611 following *distributions of travel distances and residence times*, which can then be characterized
612 by various (often power law) probability density functions.

613 **2.4 Groundwater systems**

614 As noted in Sect. 1, analysis of groundwater systems has developed largely independently
615 of investigation of catchment systems, although it, too, developed originally as a large
616 deterministic engineering discipline around the traditional task of water supply for domestic
617 and agricultural use. It was only in the 1980’s that “stochastic” (probabilistic and statistical)
618 techniques began to be implemented extensively, to account for the many uncertainties
619 associated with aquifer structure and hydraulic properties that control the flow of
620 groundwater. In parallel, significant interest (and concern) with water quality and
621 environmental contamination in groundwater systems only entered the research community’s
622 consciousness in the 1980s, although some pioneering laboratory experiments and field
623 measurements were initiated from the late 1950s.

624 It is worth noting, too, that the methods and models applied in groundwater research
625 developed independently and separately from research on catchment systems (Sect. 1). The
626 only partial connection or “integrator” has traditionally been with aquifer connections to the
627 vadose zone (or critical zone, discussed in Sect. 2.3). Another connection between surface
628 water and groundwater systems, though not generally recognized as such, has been analysis of
629 water flow, and to a lesser extent chemical species transport, in the hyporheic zone. The
630 hyporheic zone can be defined as the region of sediment and subsurface porous domain below
631 and adjacent to a streambed, which enables mixing of shallow groundwater and surface water.
632 (e.g., Haggerty et al, 2002).

633 To quantify chemical transport, landmark laboratory experiments (e.g., Aronofsky and
634 Heller, 1957; Scheidegger, 1959) measured breakthrough of conservative (non-reactive)
635 chemical tracers through columns of sand. These measurements underpinned theoretical

636 developments, based also on concepts of Fickian diffusion, which led to consideration of the
637 classical advection-dispersion equation. Since that time, the advection-dispersion equation –
638 and variants of it – have been used extensively to quantify chemical transport in porous
639 media. However, as thoroughly discussed in Berkowitz et al. (2006), solutions of the
640 advection-dispersion equation have repeatedly demonstrated an inability to properly match
641 results of extensive series of laboratory experiments, field measurements, and numerical
642 simulations. These findings naturally lead to the conclusion that the conceptual picture
643 underlying the advection-dispersion equation framework is insufficient; as detailed in Sect.
644 2.2, the soil physics community arrived at a similar conclusion. Stochastic variants of the
645 advection-dispersion equation, and implementation of multiple-continua, advection-dispersion
646 equation formulations (including mobile-immobile models) have been used to provide
647 insights into factors that affect chemical transport – particularly given uncertain knowledge of
648 detailed structural and hydraulic aquifer properties – but they have been largely unable to
649 capture measured behaviours of chemical transport. This observation is largely in line with
650 what we reported for the critical zone.

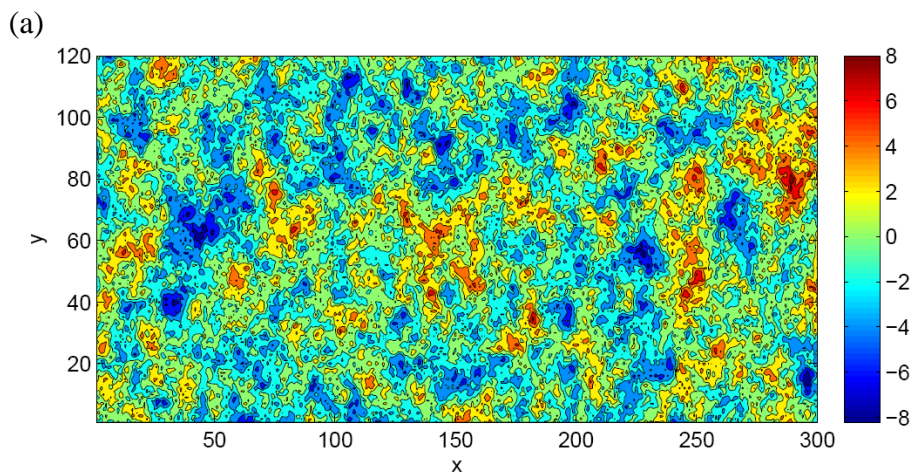
651 The first key is to recognize that heterogeneities are present at all scales in groundwater
652 systems, from sub-millimetre pore scales to the scale of an entire aquifer. Indeed, use of the
653 term “heterogeneities” refers to varying distributions of structural properties (e.g., porosity,
654 presence of fractures and other lithological features), hydraulic properties (e.g., hydraulic
655 conductivity), and – in the case of chemical transport (a general term used here and
656 throughout to denote migration of chemical (and/or microbial) components) – variations in
657 the biogeochemical properties of the porous domain medium. The second key is to recognize
658 that these variations in distributions, at all scales, deny the possibility of obtaining complete
659 knowledge of the aquifer domain in which fluids and chemical species are transported. A third
660 key, when considering chemical transport (and transport of stable water molecule isotopes), is
661 to recognize that chemical species are subject to several critical transport mechanisms and
662 controls, in addition to advection, that do not affect flow of water – molecular diffusion,
663 dispersion, and reaction (sorption, complexation, transformation) – so that chemical migration
664 through an aquifer is influenced strongly by aquifer heterogeneities and initial/boundary
665 conditions. Extensive analysis of high-resolution experimental measurements and numerical
666 simulations of transport demonstrate that small-scale heterogeneities can significantly affect
667 large-scale behaviour, and that small-scale fluctuations in chemical concentrations do not
668 simply average out and become insignificant at large scales.

669 As discussed in the preceding sections, preferential pathways are ubiquitous and affect
670 both water and chemical species, resulting from system heterogeneity. To be more specific,
671 (local) hydraulic conductivities vary in space over orders of magnitudes, even within
672 distances of centimetres to meters, and these variations ultimately control patterns of fluid and
673 chemical movement. The resulting patterns of movement in these systems involve highly
674 ramified preferential pathways for water movement and chemical migration. To illustrate
675 these points, consider the hydraulic conductivity (K) and preferential pathway maps shown in
676 Fig. 4a; see Edery et al. (2014) for full details.

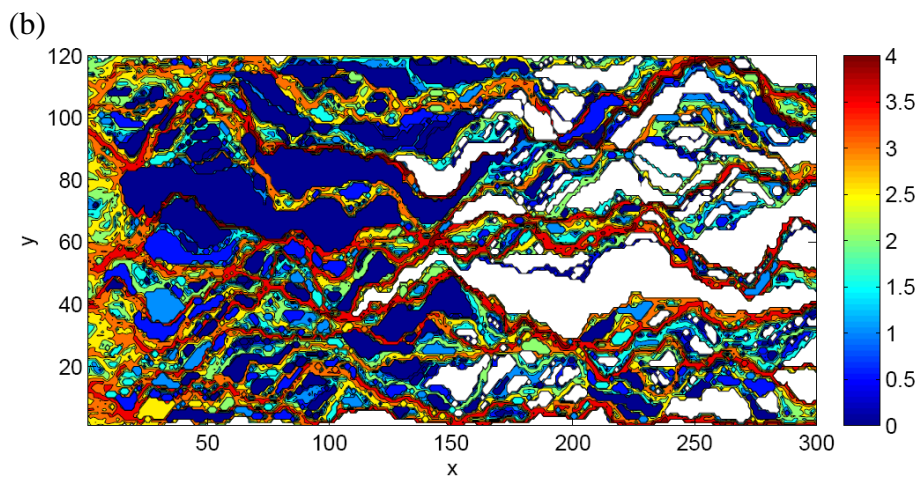
677 Figure 4a shows a numerically-generated, two-dimensional domain measuring 300×120
678 discretized into grid cells of uniform size (0.2 units). The K -field shown here was generated as
679 a random realization of a statistically homogeneous, isotropic, Gaussian $\ln(K)$ field, with

680 $\ln(K)$ variance of $\sigma^2 = 5$. Fluid flow through this domain was solved at the Darcy level by
681 assuming constant head boundary conditions on the left and right boundaries, and no-flow
682 horizontal boundaries; the hydraulic head values determined throughout the domain were then
683 converted to local velocities, and thus streamlines. Conservative chemical transport was
684 determined using a standard Lagrangian particle tracking method, with 10^5 particles
685 representing the dissolved chemical species. Particles advanced by advection along the
686 streamlines and molecular diffusion (enabling movement between streamlines), to generate
687 breakthrough curves (concentration vs. time) at various distances along the domain. Figure 4b
688 shows particle pathways through the domain, wherein the number of particles visiting each
689 cell is represented by colours. The emergence of distinct, limited particle preferential
690 pathways from inlet boundary to outlet boundary is striking. Notably, too, there are significant
691 regions that remain free of particles (the white regions in Fig. 4b), and preferential pathways
692 are confined and converge between low conductivity areas. Even more striking is set of even
693 sparser preferential pathways shown in Fig. 4c: here, only cells, which were visited by at least
694 0.1% of all injected particles, are shown. In other words, 99.9% of all chemical species
695 migrating through the domain shown in Fig. 4a advance through a limited number and spatial
696 extent of preferential pathways. It is significant, too, that the preferential pathways comprise a
697 combination of higher conductivity cells the paths, but also some low conductivity cells, as
698 reported also in Bianchi et al. (2011); see Sect. 3.1 for further discussion of this behaviour.

699
700
701

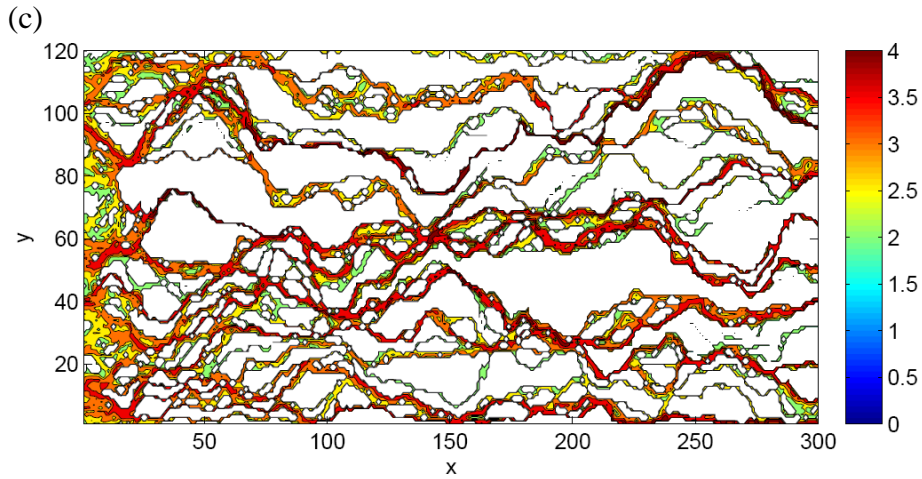


702
703



704

705

706
707

708 **Figure 4 (a)** Spatial map showing a sample hydraulic conductivity (K) field generated
 709 statistically (right side bar shows scale of $\ln(K)$). **(b)** Spatial map showing particle paths
 710 through the domain, for overall hydraulic gradient (water flow) from left to right. “Particles”
 711 representing dissolving chemical species are injected along the left vertical boundary and
 712 followed through the domain. White regions indicate where *no* particles “visit” (interrogate)
 713 the domain. Blue regions have only a small number of particle visitations. Red regions have
 714 significant particle visitations. Note that the colour bar is in \log_{10} number of particles. **(c)**
 715 Spatial map showing particle paths *preferential* particle paths, defined as paths through cells
 716 (underlying subdivisions in the domain, each with a different K value as shown in plot (a)
 717 above) that each contain a “visitation” of a minimum of 0.1% of the total number of particles
 718 in the domain. Note that the colour bar is in \log_{10} number of particles (after Edery et al.,
 719 2014; Copyright 2014, with permission from the American Geophysical Union).

720

721 Thus, it is clear that the groundwater systems incorporate regions of water – distributed
 722 throughout the domain – that may have very different chemical signatures, even in close
 723 proximity to each other. Moreover, these regions can be relatively stable over time, modified
 724 only by the extent of chemical diffusion into and out of the “immobile” regions.

725 In accord with our definition of spatial organisation in Sect. 1, we propose the use of
 726 Shannon entropy H (bits) to quantify the degree of spatial organisation in the flow pattern in
 727 Fig. 4c. To this end, we define the discrete probability density distribution to find a particle in
 728 a grid element, Δy_i , at the inlet ($x=0$) and at the outlet ($x=300$) of the flow domain, based on
 729 the numbers of particles that entered/left the domain through the corresponding grid cells
 730 divided the total number of particles that entered/left the domain N_{in}/N_{out} , as follows:

731

$$732 \quad p(x = 0, \Delta y_i) = \frac{n(\Delta y_i, x=0)}{N_{in}}; \quad p(x = 300, \Delta y_i) = \frac{n(\Delta y_i, x=300)}{N_{out}} \quad (\text{Eq. 5})$$

733

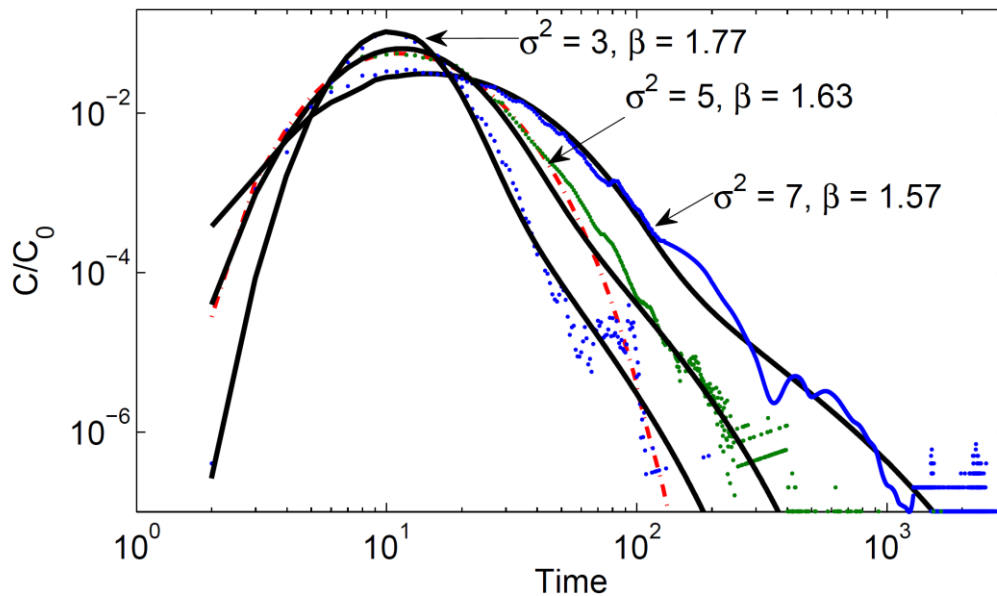
734 where $p(x=0, \Delta y_i)/p(x=300, \Delta y_i)$ are probabilities that particle entered/left the domain at Δy_i ,
 735 $n(x=0, \Delta y_i)/n(x=300, \Delta y_i)$ are the numbers of particles that entered/left the domain at Δy_i .
 736 Using these probability distributions, we calculate the respective Shannon entropy values
 737 defined as follows:

738

$$738 \quad H = -\sum p_i \log_2(p_i) \quad (\text{Eq. 6})$$

739

740 The Shannon entropy of the uniform input distribution, with 6.9 bits, corresponds to an
 741 entropy maximum. Preferential flow reduced this to $H = 3.58$ bits at the outlet, which reflects
 742 a release of chemicals that is much more organised in space. Note that a well-mixed
 743 advective-dispersive pattern would maximise the entropy at the outlet, as the concentration
 744 would be constant along the y coordinate. Considering now arrival times of chemical species
 745 at the domain outlet boundary, Fig. 5 shows the relative concentration (C/C_0) vs. time –
 746 breakthrough curves – for three degrees of domain heterogeneity ($\ln(K)$ variance). (The well-
 747 mixed case would maximise the entropy at the outlet, corresponding to a CTRW fit with $\beta = 2$
 748 in Fig. 5.) It is evident that the chemical transport in this domain displays “non-Fickian” (or
 749 “anomalous”) transport, in the sense that late-time (long tail) arrivals are registered at the
 750 measurement plane. Furthermore, Fickian-based advection-dispersion equation models clearly
 751 fail to quantify such behaviour (Fig. 5). However, Fig. 5 shows solutions – based on the
 752 continuous time random walk (CTRW) framework – that do effectively describe the chemical
 753 transport. The CTRW framework and governing transport equations are detailed in Sect. 3.3.
 754
 755



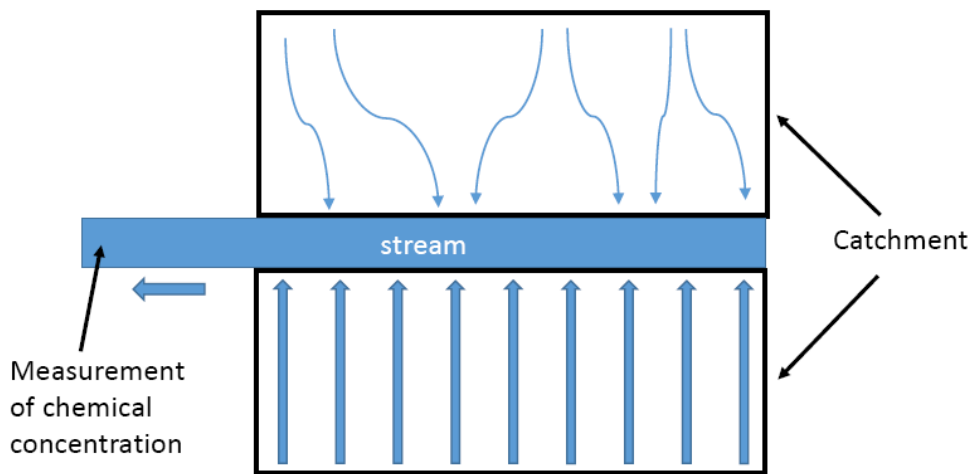
756
 757 **Figure 5** Breakthrough curves (points) for three $\ln(K)$ variances ($\sigma^2 = 3, 5, 7$; 100 realizations
 758 each), at the domain outlet ($x = 300$ length units), and corresponding CTRW fits (curves).
 759 Also shown is a fit of the advection-dispersion equation (dashed-dotted curve), for $\sigma^2 = 5$.
 760 See Sect. 3.3 for further discussion and explanation of β . All values are in consistent, arbitrary
 761 length and time units (after Ederly et al., 2014; Copyright 2014, with permission from the
 762 American Geophysical Union).

763 3 MERGING TREATMENT OF SURFACE WATER AND 764 GROUNDWATER SYSTEM TRANSPORT DYNAMICS

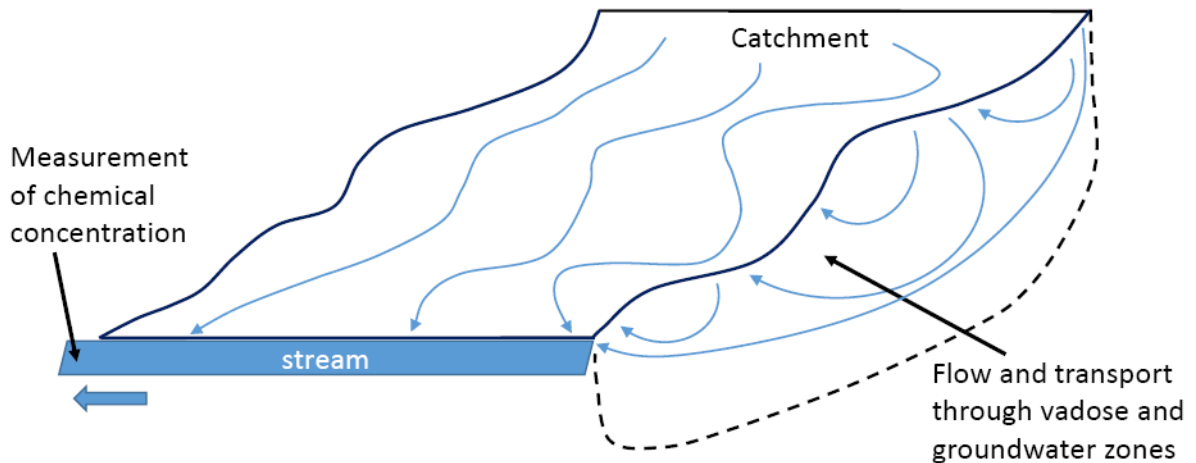
765 3.1 Conceptual pictures, travel times, and mixtures of water with different chemical 766 signatures

767 Clearly, any quantitative model of fluid flow and chemical transport in a catchment must
 768 first define a conceptual picture. In the context of the discussion in Sects. 2 and 3 that led us

769 to this point, we require a picture that accounts naturally for overland and interacting
 770 subsurface flow and transport, recognizing the ubiquity of preferential pathways and a broad
 771 (and often different) distributions of fluid and chemical travel times. Moreover, any such
 772 conceptual picture also requires definition of the available measurement benchmark against
 773 which a quantitative model can be compared. In the case of catchments, a common
 774 measurement is that of chemical arrival times at a downstream sampling point in a catchment
 775 stream that drains and exits the catchment. Thus, the dynamics of fluid flow and chemical
 776 transport in a fully three-dimensional (or simplified two-dimensional overland) catchment are
 777 often represented by measurements in an effective, spatially averaged one-dimensional
 778 system. (Of course, higher resolution, multidimensional (in space) measurements, if available,
 779 should also be considered in a quantitative model!)



781
 782 (a)
 783



784
 785 (b)
 786

787 **Figure 6** Conceptual pictures of water flow and chemical transport in catchments under a
 788 pulse of rainfall over the entire catchment. Each curved arrow (or idealized straight arrow)
 789 indicates a different path, each of which embodies different travel times through the system
 790 until reaching the stream. Note that each preferential pathway carrying water and chemical

791 species may be purely overland, or include interactions and advance within soil layers
792 (partially saturated, or vadose, zone) and saturated groundwater systems. **(a)** Schematic
793 showing idealized 2D catchment area. Arrows through two rectangular regions of catchment
794 indicate a range of preferential pathways carrying water and chemical species. **(b)** Schematic
795 showing idealized 3D catchment area, under a pulse of rainfall over the entire catchment.
796

797 Figures 6a and 6b show, schematically, 2D and 3D conceptualizations of preferential
798 pathways, with associated varying travel times through the catchment, for both fluid flow and
799 chemical transport. We stress here – and as discussed below in Sect. 3.3 – that the larger
800 scale, effective (or “characteristic”, or average) fluid velocities and chemical species transport
801 velocities need not be identical. For example, using a conceptual mixing model, Hrachowitz
802 et al. (2015) showed that chloride transport can be slower than water transport. In fact, these
803 two velocities are rarely the same, as a consequence of the ubiquity of preferential pathways
804 for water and migrating chemical species in any surface water and/or soil-aquifer domain.
805 Because of these pathways, regions of higher and lower hydraulic conductivity (fluid and
806 chemical mobility) – and thus the entire system – interrogated by water and chemical species
807 differ. While both water molecules and chemical species are subject to diffusive and
808 dispersive transport mechanisms, in addition to advection, these effects are clearly identifiable
809 for chemical species, while they are undistinguishable for individual water molecules. Thus
810 the effects of diffusion and dispersion on “bulk water” transport, e.g., into and out of low
811 conductivity zones, are invisible and irrelevant, while chemical species retained in these same
812 zones can have a major impact on the overall (and “average”, centre of mass) advance of a
813 chemical plume. These effects are also visible and relevant for isotopes of the water molecule,
814 as deuterium and tritium are subject to self-diffusion in water. The latter implies that isotope
815 concentrations between old and new water pockets in the subsurface might mix diffusively,
816 even when there is no physical mixing between these waters. Hence, the relation between
817 water age and its isotopic decomposition is not straightforward.

818 The conceptual picture discussed here is our basis for arguing that we should expect to
819 find distributions of travel times and mixtures of water with different chemical signatures, *at*
820 *all scales*. Moreover, these considerations align well with our reflections in Sect. 2 and key
821 studies in catchment hydrology, which clearly recognize the occurrence of wide distributions
822 of water and chemical travel times, and long-term chemical persistence in water catchment
823 storage (e.g., Niemi, 1977; Botter et al., 2010, 2011; Hrachowitz et al., 2010; McDonnell and
824 Beven, 2014; Kirchner, 2016).

825 As pointed out in Sect. 2, several studies in recent years have specifically reported the
826 presence of water bodies (or pockets, or regions, depending on scale), with different chemical
827 compositions and isotopic signatures, that are in close proximity or even “overlapping” (in
828 some sense). Some authors use the term “two water worlds” – immobile and mobile – in this
829 context (e.g., McDonnell, 2014) to describe the different sources of water returned to the
830 atmosphere by vegetation transpiration and released to streams; we stress again that our use of
831 the term in this paper highlights the different catchment hydrology and groundwater
832 communities and associated research tools. In light of the discussion in Sect. 2, we stress here
833 that the conceptual picture to explain spatially and temporally varying chemical compositions
834 (in subsurface, soil, sediment and aquifer systems), and associated uptake by vegetation, is
835 subtle. We question the conceptualization of two (or more) *separate, fully compartmentalized*

836 mobile and immobile regions of water and chemicals. We argue that mobile and immobile
837 regions are more appropriately considered as overlapping continua or ensemble/effective
838 averages, as those are found at all scales from pores to hundreds of meters (e.g., Turton et al.,
839 1995; Collins et al., 2000; Gouet-Kaplan and Berkowitz, 2011; recall Sect. 2.3). With the
840 occurrence of mixtures of travel times and waters having different chemical signatures at all
841 scales, we argue that it is preferable to think in terms of time, such that there is a range of
842 overlapping temporal (transition time) distributions that each contribute to the overall, large-
843 scale fluid flow and chemical transport. This leads naturally to the CTRW framework.

844 **3.2 Space vs. time: the travel time perspective of transport**

845 It is critical to point out that in the figures shown above in Sects. 2.3 and 2.4, the
846 *residence times* of water and chemicals are the key factors that determine transport behaviour.
847 This leads to the continuous time random walk (CTRW) framework, which operates more (or
848 at least equally!) in terms of time than in terms of space (see Sect. 3.2). To introduce CTRW,
849 in the context of the pathway “self-organisation” shown in Fig. 5c, we demonstrate the
850 importance of thinking in terms of *time* rather than *space*. Consider the simple example of
851 driving a distance of 100 km; we consider a scenario in which we travel 50 km at 1 km/h, and
852 then 50 km at 99 km/h. The average speed of travel, in terms of *space* (distance), is
853 determined as follows: given that we travelled 50 km at each of two speeds, the average speed
854 is $(1 + 99) / 2 = 50$ km/h. Thus, with this calculation, the total time to travel 100 km “should”
855 be 2 h. However, the *actual* time taken to travel this distance – 50 km at 1 km/h, and then 50
856 km at 99 km/h – is 50.5 h. In other words, traditional (but incorrect!) conceptual spatial
857 thinking highlights the erroneous effects of focusing only on *spatial* heterogeneity and
858 quantification based only on spatial characteristics.

859 In a similar analogy, it is sometimes faster to pass through a bottleneck region (e.g., drive
860 for a short time through a very narrow and slow road) to ultimately reach a fast highway,
861 rather than to travel at medium speed along a road for an entire journey.

862 Another aspect related to misplaced emphasis on spatial heterogeneities, is also noted
863 here. Referring again to the preferential pathways show in Fig. 4c, it is seen that these
864 pathways actually contain some low hydraulic conductivity (K) regions as well! This can be
865 explained most easily, conceptually, in terms of one-dimensional pathways. Consider a
866 number of high and low K cells in series, [3 3 3 3 3] vs. [6 6 1 6 6], where the
867 effective/average K is given by the harmonic mean. While a [3 3 3 3 3] series may appear to
868 enable a greater volumetric flow rate than a [6 6 1 6 6] series, due to the “bottleneck” low K
869 value in the centre, both series in fact have the same harmonic mean ($=3$) and conduct fluid
870 equally well.

871 A similar argument can be applied to analysis of land topography and surface water flow.
872 The “high resistance” (in principle, but not necessarily), localized small ‘humps of roughness
873 elements’, and surface tension effects – analogous to the low K cells given in the previous
874 paragraph – can be overcome, to allow development of preferential pathways that do not
875 always follow the path of steepest descent in terms of surface topography. There are thus
876 small bypassing effects. Moreover, there is flow/transport from land surface into the
877 subsurface (e.g., hyporheic zone), which also “bypasses” localized small “humps” in the land
878 surface and allows fluid connection/communication further downstream (along a pathway).

879 As a consequence, we argue that it is misleading to place undue focus on the high resistance
880 (or surface “hump”) bottlenecks; rather, it should be recognized that entire “high K” or
881 “potential” regions for flow are often unsampled or barely sampled by flowing water and
882 chemicals, at least over moderate time scales.

883 To further expand on the link between spatial and temporal heterogeneity, we point out
884 that the key is to think in space-time and complementary manifestations of heterogeneity of
885 preferential flow. We already showed that a heterogeneous preferential flow pattern implies
886 that chemical species leave the system at distinct locations, which implies a strong reduction
887 in Shannon entropy, as shown in Sect. 2.4 for the example of Ederly et al. (2014). When
888 observed at a fixed outlet, these heterogeneous flow patterns translate into signatures of the
889 breakthrough curve. Again, this can be quantified through the corresponding deviations from
890 a Fickian breakthrough curve, which is the maximum entropy travel time distribution,
891 reflecting well-mixed, advective-dispersive transport (Tefry et al., 2003). The overall key
892 messages of Sect. 3 are that (a) CTRW is consistent with the advection-dispersion equation
893 and advances beyond it, particularly in terms of capturing dispersion and tailing effects, and
894 (b) the power law exponent is related to porous media characteristics as well as the flow
895 conditions, although this relation is not unique. Nevertheless, the opportunity arises to at least
896 partly constrain spatial signatures of the subsurface from temporal ones with uncertainty. This
897 non-uniqueness is another manifestation of the inherent equifinality problem, when reviewing
898 model concepts in catchment science in Sect. 2.1.

899 In the next section, we adopt a temporal framework to introduce continuous time random
900 (CTRW) theory, which is the basis of our proposed means to unify quantification of
901 groundwater and surface water transport dynamics.

902 **3.3 Continuous Time Random Walks: Theory**

903 Preferential flow leads to non-Fickian (or “anomalous”) travel time distributions,
904 characterised by rapid breakthrough and/or long tailing of chemical species through
905 heterogeneous domains. The CTRW framework is well suited to deal with this in a manner
906 that is consistent with microscale physics, and it steps beyond the advection-dispersion
907 equation approach. This might also offer opportunities to understand SAS from a bottom up
908 perspective, as age ranked storage relates to the integral of the travel time distribution across
909 all ages.

910 Detailed descriptions of CTRW can be found in, e.g., Berkowitz et al. (2006, 2016). Here,
911 we present only a brief outline of the essential elements. The CTRW framework is based on
912 direct incorporation of the distribution of flow field fluctuations and thus of the fluctuations in
913 concentrations of transported chemicals. As such, the CTRW is a time-nonlocal approach that
914 can quantify chemical transport over a range of length (and time) scales, and address other
915 processes such as chemical reactions.

916 From a microscale of view, “particles”, representing dissolved chemical species, are used
917 to treat chemical transport; each particle undergoes spatiotemporal transitions – “transitions
918 (or steps) in a random walk” – that encompass both displacement due to structural
919 heterogeneity and the time taken to make each particle movement. Unlike other approaches,
920 the formulation focuses on retaining the full distribution of transition times. Thus, CTRW
921 defines a probability density function (PDF), $\psi(\mathbf{s}, t)$, of a random walk that couples the spatial

922 displacement \mathbf{s} and time t of the transition. As shown in Dentz et al. (2008), it is convenient
 923 and generally applicable (but not obligatory) to use the decoupled form $\psi(\mathbf{s}, t) = p(\mathbf{s})\psi(t)$,
 924 where $\psi(t)$ is the probability rate for a transition time t between sites, and $p(\mathbf{s})$ is the
 925 probability distribution of the length of the transitions. We stress here that the particle
 926 *transition* time distribution represents the PDF of times for any given particle transition over
 927 the distance \mathbf{s} , while the *travel* time distribution – also called a “first passage time
 928 distribution” – discussed above and below is the PDF of arrival times (an “overall response”)
 929 through a catchment, soil column, or aquifer at a measurement point or plane. A breakthrough
 930 curve, representing the concentration of all particles arriving at a control/measurement point
 931 (or plane) over time, can then be determined by calculating the average travel (first passage)
 932 times of all particles exiting boundary of the flow domain. Thus, the *transition* time
 933 distribution – however chosen – is the PDF underlying the resulting solution (which can be
 934 characterized in terms of the breakthrough curve, as well as *travel* time, or first passage time,
 935 distribution, as well as in terms of spatial profiles and moments) of the governing transport
 936 equation; see Sect. 3.4 for further discussion. [Note: Regarding first passage time distributions
 937 and breakthrough curves, a subtlety must be kept in mind, namely, that the breakthrough
 938 curve is equal to the first passage time distribution if one measures it at an absorbing
 939 boundary (“exiting the flow domain” could be represented by an absorbing boundary).
 940 Otherwise, the flux-averaged concentration is obtained from the net flux across a boundary
 941 (Simmons, 1982; or Appendix of Dentz et al., 2004). Nevertheless, the analytical expressions
 942 for the first passage time distribution and flux concentration are equal under certain boundary
 943 conditions.]

944 The defining transport equation is equivalent to a generalized master equation (GME),
 945 which is essentially a mass balance equation in space and time. Using a Taylor expansion, the
 946 GME can be transformed into the continuum version (ensemble-averaged system) of the
 947 CTRW, in the form of an integro-partial differential equation:

$$948 \quad \frac{\partial c(\mathbf{s}, t)}{\partial t} = \int_0^t dt' M(t - t') [-\mathbf{v}_\psi \cdot \nabla \tilde{c}(\mathbf{s}, t') + \mathbf{D}_\psi : \nabla \nabla \tilde{c}(\mathbf{s}, t')] \quad (\text{Eq. 7})$$

950
 951 for the normalized concentration $c(\mathbf{s}, t)$, where M is a memory function, the transport velocity
 952 \mathbf{v}_ψ and the generalized dispersion \mathbf{D}_ψ are defined in terms of the first and second moments of
 953 $p(\mathbf{s})$, and with the dyadic symbol $:$ denoting a tensor product. In Laplace space, (1) becomes

$$954 \quad u \tilde{c}(\mathbf{s}, u) - c_o(\mathbf{s}) = -\tilde{M}(u) [\mathbf{v}_\psi \cdot \nabla \tilde{c}(\mathbf{s}, u) - \mathbf{D}_\psi : \nabla \tilde{c}(\mathbf{s}, u)] \quad (\text{Eq. 8})$$

956
 957 where the memory function $\tilde{M}(u) \equiv \bar{t} u \tilde{\psi}(u) / [1 - \tilde{\psi}(u)]$, \bar{t} is a characteristic time, and with
 958 \sim denoting Laplace space and u denoting the Laplace variable. Note that this continuum
 959 formulation contains a nonlocal-in-time convolution, in terms of the memory function.

960 In contrast to the classical advection-dispersion equation (see Eq. (11), below), the
 961 “transport velocity,” \mathbf{v}_ψ is in principle distinct from the “average fluid velocity,” \mathbf{v} . This is
 962 because chemical transport is “clearly identifiable”, subject to diffusive and dispersive
 963 mechanisms (recall the discussion following Fig. 6), so that the effective, overall transport
 964 (i.e., a “characteristic” velocity) of chemical may be faster or slower than the average fluid

965 velocity. We point out, moreover, that residence times are a key characterisation, as they
 966 generally differ for water and chemical species. To illustrate, it is sufficient to recognise that
 967 the preferential flow paths themselves are generally stable when the overall hydraulic gradient
 968 changes (unless dealing with significant changes or turbulent flow), so that the residence time
 969 dictates the relative influence of diffusion and chemical movement into and out of less mobile
 970 zones, which ultimately affects breakthrough curves (Berkowitz and Scher, 2009).

971 It is critical to recognize that the occurrence of “rare events” – even a small proportion of
 972 chemical species migrating extremely slowly in some regions, and/or being repeatedly
 973 trapped and released of slow regions over a series of spatial transitions – are sufficient to lead
 974 to anomalous transport and extremely long “average” chemical transport times (Berkowitz et
 975 al., 2016). Thus, it is important to differentiate between “average” (recall Sect. 3.1) and
 976 “effective” transport of “most” particles. Indeed, we emphasise, too, that the effects of these
 977 “rare events” are deeply significant: they do not simply average out, but rather propagate to
 978 larger time and space scales.

979 With the decoupled form $\psi(\mathbf{s}, t) = p(\mathbf{s})\psi(t)$, the transition time distribution, $\psi(t)$, is thus at
 980 heart of the CTRW framework, and its form determines the memory function; the role of $p(\mathbf{s})$
 981 on non-Fickian transport is relatively insignificant as long it has a compact (finite) range
 982 (Dentz et al., 2008). As discussed in detail (e.g., Berkowitz et al., 2006, 2016), it is expedient
 983 to define (t) as a truncated power law (TPL), which enables an evolution to Fickian
 984 behaviour:

$$985 \quad \psi(t) = \frac{n}{t_1} \exp(-t/t_2) / (1 + t/t_1)^{1+\beta} \quad (\text{Eq. 9})$$

987 for $0 < \beta < 2$, with the normalization constant

$$989 \quad n \equiv (t_1/t_2)^{-\beta} \exp(-t_1/t_2) / \Gamma(-\beta, t_1/t_2) \quad (\text{Eq. 10})$$

991 and with $\Gamma(-\beta, t_1/t_2)$ denoting the incomplete Gamma function (Abramowitz and Stegun,
 992 1970). This functional form of $\psi(t)$ has been particularly successful in interpreting a wide
 993 range of laboratory and field observations, as well as numerical simulations. We chose the
 994 characteristic time appearing in the memory function to be t_1 , which represents the onset of
 995 the power law region. The truncated power law form of $\psi(t)$ behaves as a power law
 996 proportional to $(t/t_1)^{-1-\beta}$ for transition times in the range $t_1 < t < t_2$; $\psi(t)$ decreases
 997 exponentially for transition times $t > t_2$. Thus, the TPL enables quantification of non-Fickian
 998 transport, with a finite (sufficiently small) t_2 , it facilitates (where appropriate) a longer-time,
 999 smooth evolution to Fickian transport. We note, too, that the CTRW framework also
 1000 simplifies (e.g., Berkowitz et al., 2006, 2016) to specialized subsets of non-Fickian transport
 1001 behaviour embodied within, e.g., multirate mass transfer (Haggerty and Gorelick, 1995) and
 1002 fractional derivative (Zhang et al., 2009) formulations.

1004 It is important to recognize, too, that specification of a pure exponential form for $\psi(t)$,
 1005 namely $\psi(t) = \lambda \exp(-\lambda t)$, with mean $1/\lambda$, and/or choice of $\beta > 2$, reduces the CTRW transport
 1006 Eq. (7) to the classical advection-dispersion equation, given in a general form as

1007

1008
$$\frac{\partial c(\mathbf{s}, t)}{\partial t} = -\mathbf{v}(\mathbf{s}) \cdot \nabla c(\mathbf{s}, t) + \nabla \cdot [\mathbf{D}(\mathbf{s}) \nabla c(\mathbf{s}, t)]$$
 (Eq. 11)

1009

1010 where $\mathbf{v}(\mathbf{s})$ is the velocity field and $\mathbf{D}(\mathbf{s})$ is the dispersion tensor.

1011 It is thus clear that the power law exponent β in $\psi(t)$ characterises the local disorder of the
 1012 system and the degree of non-Fickian transport as an integral, temporal fingerprint in the
 1013 breakthrough curves. This reflects the effect of a strongly localised preferential movement of
 1014 chemical species on travel times (recall Fig. 4), caused by the pattern of local driving
 1015 gradients and hydraulic conductivity. Because the particle movement is clearly organised in
 1016 *space*, we suggest that this might be seen as self-organisation: local disorder is manifested in
 1017 deviation from advective-dispersive transport, which leads to *non-local*, organised dynamic
 1018 behaviour in *time* at the system scale. This implies that the CTRW framework provides a
 1019 means to quantify the integral, temporal fingerprint of spatially organised preferential flow
 1020 through the power law exponent β and the related distance from a Gaussian travel time
 1021 distribution.

1022 The CTRW transport equation, in partial differential equation form, can be solved in
 1023 Laplace space (Cortis and Berkowitz, 2005) as well as in real space (Ben-Zvi et al., 2019).
 1024 One can also solve the transport equation by implementing various particle-tracking
 1025 formulations. This was done, for example, to obtain the fits to the long-tailed breakthrough
 1026 curve displayed in Fig. 6. Particle tracking (PT) approaches offer an efficient numerical tool
 1027 to treat a variety of chemical transport scenarios (for both conservative and reactive chemical
 1028 species). They are particularly well-suited to accounting for pore-scale to column-scale
 1029 dynamics. “Particles” (representing chemical mass) advance by sampling transitions in space
 1030 and time from the associated CTRW distributions. We emphasize that this PT approach can
 1031 be employed to treat both advection-dispersion equation (Fickian, normal transport) and
 1032 CTRW (non-Fickian, anomalous transport) formulations, via appropriate choice of
 1033 (exponential or power law, respectively) $\psi(t)$.

1034 The efficacy and relevance of the CTRW framework has been demonstrated extensively
 1035 for subsurface chemical transport (Berkowitz et al., 2006, 2016; Berkowitz and Scher, 2009;
 1036 and references therein), from pore to aquifer scales, on the basis of extensive numerical
 1037 simulations, laboratory experiments and field measurements. The formulation for chemical
 1038 transport is general and robust over length scales ranging from pore to field, for different flow
 1039 rates within the same domain, for chemically-reactive species, and even for time-dependent
 1040 velocity fields (Nissan et al., 2017).

1041 To conclude this section, and bridge to discussion that follows in the next section, we
 1042 point out here that, the *curved power law* form can in some cases be a useful representation
 1043 rather than the truncated power law (TPL), Eq. (9), as shown by Nissan and Berkowitz
 1044 (2019). In this case, we write $\psi(t)$ as a curved power law function (Chabrier, 2003)

1045

1046
$$\psi(t) = C_1 t^{-1-\beta} \exp(-t^*/t)$$
 (Eq. 12)

1047

1048 where $C_1 \equiv (t^*)^\beta / \Gamma(\beta)$, is the normalization constant of the probability density function and Γ
 1049 is the Gamma function. Here, t^* (a characteristic time) controls the exponential increase, while
 1050 β accounts for the power law region. It is important to note that this curved power law is an

1051 *inverse gamma distribution*, with shape parameter β and scale (or rate) parameter t^* . Note that
1052 unlike the TPL in Eq. (9), notwithstanding the exponential term in Eq. (12), there is no cut-off
1053 time that enables a transition to Fickian transport. These perspectives will be discussed in
1054 detail in Sect. 3.4.

1055 **3.4 Continuous Time Random Walks: Application to surface water systems**

1056 In the context of our discussion in Sects. 2 and 3.1, recognizing that dynamics of chemical
1057 transport in surface water and groundwater systems are at least phenomenologically and
1058 functionally/dynamically similar over enormous spatial and temporal scales, we argue there
1059 that simulations and analysis using the CTRW framework are meaningful and applicable also
1060 to quantifying the (anomalous) dynamics of chemical transport in surface water systems. In
1061 both surface water and groundwater systems, there is always “unresolved heterogeneity” (e.g.,
1062 hydraulic conductivity, structure) at all scales. Fluid and chemical inputs range from being
1063 reasonably well-defined to unknown (e.g., in terms of location and extent of a subsurface
1064 contamination leak, areal extent and space-time heterogeneities of rainfall and related stable
1065 isotope concentrations), while outputs may also be reasonably well-defined to unknown (e.g.,
1066 arrival times of a chemical species to a monitoring point downstream, such as a stream gauge,
1067 near surface spring or tile drain outlet). As a consequence, efforts to delineate preferential
1068 flow paths and quantify chemical transport must be “adjusted” (or “be appropriate”) to the
1069 level of knowledge and spatial/temporal resolution.

1070 More specifically, we note that the preferential pathways shown in Fig. 4b,c are
1071 (phenomenologically, at least) similar to those of surface water systems shown in Fig. 1,
1072 while the (temporal) breakthrough curves in Fig. 5 are similar to those determined at stream
1073 gauges and tile drain outlets. Clearly, in surface water systems, and throughout small,
1074 intermediate and large scales, there are stable regions of “water pockets” (less mobile water)
1075 that can be distinguished by strongly varying chemical (ionic, isotopic) compositions. The
1076 presence of tributaries leading to rivers in catchments demonstrates clear channelling effects
1077 and the establishment of preferential pathways (Sect. 2).

1078 Before discussing chemical transport and considering CTRW applications in the context
1079 of surface water systems, we emphasise – as described early in Sect. 3.3 – the
1080 interrelationship between transition time distributions, travel time distributions, and
1081 breakthrough curves. The *transition* time distribution, as used particularly in the context of
1082 particle tracking and random walk model formulations, is the underlying (“building block”)
1083 characterization of chemical movement in the domain. In other words, the *transition* time
1084 distribution controls the nature of the overall transport. The *travel* time distribution is
1085 obtained as the normalized histogram of the travel times (which can be based on the *transition*
1086 time distribution) over all flow paths, or in other words, the travel time is the sum of the
1087 individual transition times and the distribution is obtained by sampling over all travel times.
1088 [Note: If one integrates the travel time distribution over all particles entering the system (in
1089 space and in time), for a step input, one obtains the cumulative breakthrough curve (c vs. t).
1090 The relation between flux concentrations, pulse inputs, and breakthrough curves, relative to
1091 the first passage time distribution for a homogeneous medium, is discussed in Section 3.1 of
1092 Dentz and Berkowitz, 2003.)]

1093 In the context of these three types of quantification of chemical movement, and in light of
1094 consideration of Eqs. (3) and (6) and the analysis to follow below, we stress the fundamental
1095 importance of the underlying transition time distribution in quantifying chemical transport
1096 through an aquifer or catchment. Common formulations of the governing transport equation,
1097 particularly the advection-dispersion equation and many variants thereof, do not include an
1098 explicit accounting of the transition or travel time distributions. However, as seen from the
1099 discussion of Eq. (11), an underlying exponential transition time distribution in the CTRW
1100 transport equation leads to the advection-dispersion equation with a Gaussian breakthrough
1101 curve. In sharp contrast, in the case of a power law transition time distribution that scales as
1102 scales as $t^{-1-\beta}$, such as given in Eqs. (9) and (12), the resulting breakthrough curve for a
1103 point/pulse input also scales as $t^{-1-\beta}$, as a direct consequence of the generalized central limit
1104 theorem (e.g., Dentz and Berkowitz, 2003, Eqs. (73) and (82)). For a step input, the scaling is
1105 $t^{-\beta}$, because it can be obtained from the point by integration in time.

1106 CTRW has also been applied in some partially saturated soil-water systems, which further
1107 strengthens the connection of CTRW to surface water systems; as discussed in Sects. 2 and
1108 3.1 (Figs. 4a,b), surface water flow and associated chemical transport are not purely overland
1109 processes, but involve coupled interactions with the partially saturated (vadose) zone (Sect.
1110 2.3) and groundwater zone (Sect. 2.4).

1111 Indeed, CTRW methods (and subsets) have already been applied in some sense, at least
1112 qualitatively, to interpret anomalous transport in various surface water system scenarios. For
1113 example, Boano et al. (2007) used CTRW to quantify chemical transport in a stream,
1114 accounting for fluid-chemical interactions with the underlying sediment (i.e., the hyporheic
1115 zone). Other studies have recorded power law and related multirate rate mass transfer
1116 dynamics for chemical transport in stream and catchment systems (e.g., Haggerty et al., 2002;
1117 Gooseff et al., 2003). These authors note, in particular, that the hyporheic zone exhibits an
1118 enormous range of time scales over which chemical exchange can occur, with significant
1119 amounts of chemical species being retained over extremely long times.

1120 However, while full application of CTRW to catchment-scale surface water systems has
1121 not been reported to date, there are additional strong indications that it is applicable. We point
1122 out two key aspects to support this claim, from the catchment hydrology literature. As
1123 discussed in Sect. 2.2.3, previous studies used a gamma distribution to parameterize travel
1124 time distributions (e.g., Hrachowitz et al., 2010), while more recent studies use a single or
1125 several gamma distributions to characterise StorAgeSelection functions of stream flow and
1126 evaporation. The gamma distribution, used particularly in connection with arrival times of
1127 stable isotopes at a catchment outlet (= river outlet, measurement control plane) – i.e., as a
1128 *travel* time distribution – has been applied to describe the superposition of different functions
1129 to account for time dependence (e.g., Hrachowitz et al., 2010). Related directly to this point,
1130 too, are unit hydrograph analyses that were used in the past to describe runoff concentration
1131 and flood routing, through a Nash Cascade, which is essentially a gamma distribution, as
1132 discussed also in Sect. 2.2.3. We now focus on this aspect in detail.

1133 The gamma distribution is given by

1134

1135

1136

$$P(t) = C_2 t^{-1+\beta} \exp(-t t^*), \quad (\text{Eq. 13})$$

1137

1138 where $C_2 \equiv (t^*)^\beta / \Gamma(\beta)$, or, equivalently (and for comparison to Eq. (12)),

1139

$$1140 \quad P(t) = C_3 t^{-1+\beta} \exp(-t/t^*), \quad (\text{Eq. 14})$$

1141

1142 where $C_3 \equiv 1/[(t^*)^\beta \Gamma(\beta)]$. The gamma distribution describes processes for which the waiting
1143 times between Poisson distributed events are important.

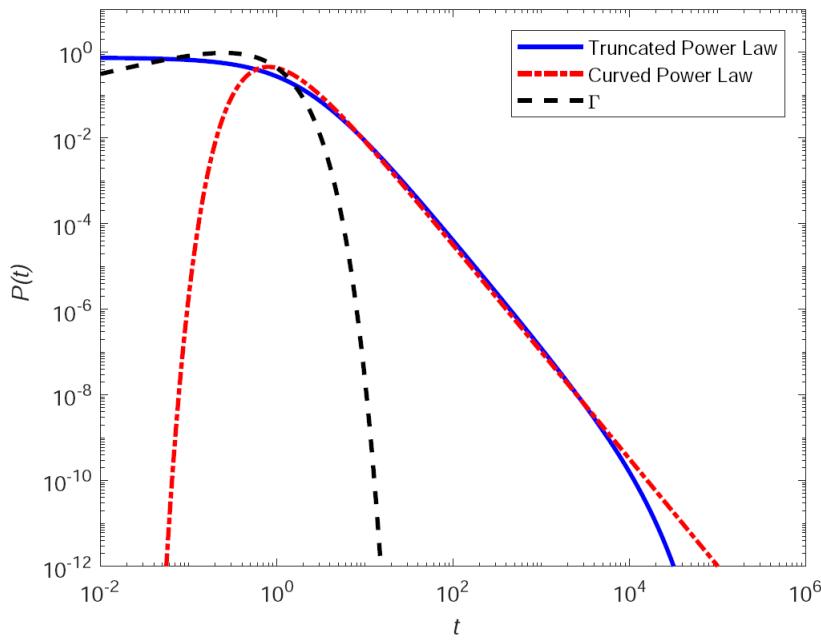
1144 In light of Sect. 2, and the discussion of transition and travel time distributions in Sect. 3.3
1145 and above, we consider what underlying *transition* time distribution leads to a gamma
1146 distributed *travel* time. Given that a sum of gamma distributed random variables can also be
1147 gamma distributed, the choice of a gamma distribution for both *transition* and *travel* time
1148 distributions is convenient. -et al., 2017).

1149 Indeed, in terms of transition time distributions, let us compare the gamma distribution in
1150 the form of Eq. (14) to the inverse gamma distribution as shown in Eq. (12). Aside from the
1151 normalisation coefficients, the inverse gamma and gamma distributions shown in Eqs. (12)
1152 and (14) differ in two fundamental ways – the power law (exponent of t) terms, $t^{-1-\beta}$ vs. $t^{-1+\beta}$
1153 and the exponential terms, $\exp(-t^*/t)$ vs. $\exp(-t/t^*)$, respectively. We stress again, as explained
1154 in Sect. 3.2, that the *inverse* gamma distribution is a power law distribution (without an
1155 exponential cut-off time to allow transition to Fickian transport), and thus one form of
1156 transition time distribution $\psi(t)$ in the CTRW formulation.

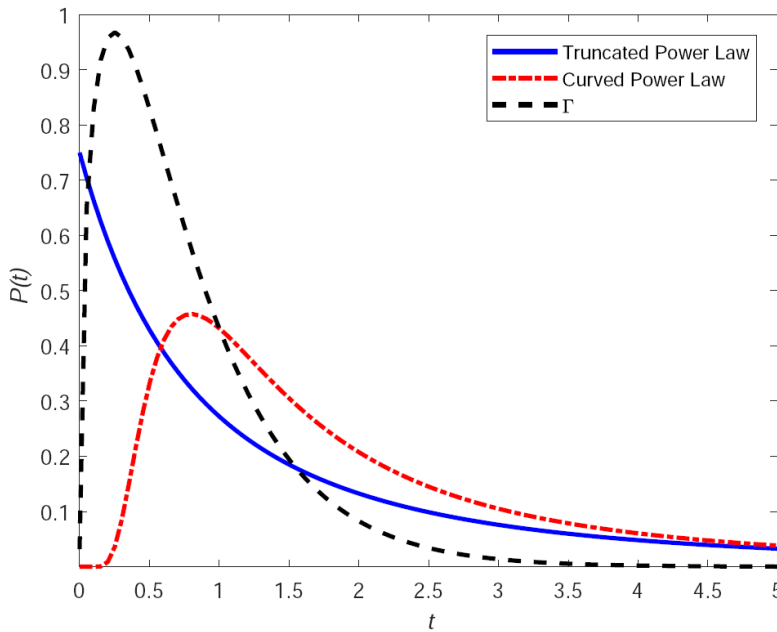
1157 We plot in Fig. 7a the truncated power law, curved power law (inverse gamma) and
1158 gamma (*transition* time) distributions, $P(t)$, for the specific parameters $\beta = 1.5$, $t_1 = 1$, $t_2 = 10^3$,
1159 $t^* = t_1$. We plot in log-log scale to emphasize the long-time portion of the transition time
1160 distribution. Figure 7b shows the same curves plotted on a linear scale, to contrast the fact that
1161 linear plots (noting the short time scale on the x -axis) do not illustrate the long-time
1162 contributions, which can have a critical effect on the overall transport behaviour. Clearly,
1163 from Fig. 7b, the gamma distribution has does not include the possibility of long times; it has
1164 an exponential cut-off to Gaussian behaviour at times larger than t^* , as the exponential term
1165 dominates the power law term when $t \gg t^*$. However, note that the power law is $t^{-1+\beta}$ rather
1166 than $t^{-1-\beta}$. The inverse gamma distribution, on the other hand, does not display an exponential
1167 cut-off, but has the same $t^{-1-\beta}$ power law scaling as the TPL.

1168 We thus conclude (recall also the conceptual picture and discussion in Sect. 3.1) that
1169 although there is no universally “right” or “wrong” choice, the gamma (*transition* time)
1170 distribution does not generally appear as a suitable “candidate” to quantify chemical transport
1171 in surface water systems, notwithstanding its empirical use in the literature. We suggest that
1172 the CTRW framework (Sect. 3.3) rests on a more physically justified conceptual picture and
1173 corresponding, coherent and robust mathematical formulation; other such frameworks and
1174 transition time distributions can of course also be considered, if justified physically. The
1175 choice of a truncated power law or inverse gamma (*transition* time) distribution is largely a
1176 function of scale. The inverse gamma distribution may better suit pore-scale (microscale)
1177 domains, where the peak of the function is important, and where ergodicity is not relevant (the
1178 cut-off is not needed). Using the truncated power law is “more” general, and better suits a
1179 variety of larger scale problems.

1180



1181 (a)



1182 (b)

1183 **Figure 7** Truncated power law, curved power law (inverse gamma distribution) and gamma
 1184 distribution, for the specific parameters: $\beta = 1.5$, $t_1 = 1$, $t_2 = 10^3$, $t^* = t_1$. **(a)** Log-log scale to
 1185 emphasise the long-time tailing behaviour. **(b)** Linear scale.

1186

1187 We now consider a specific example that demonstrates the relevance and applicability of
 1188 the CTRW framework for chemical transport in surface water systems, keeping the above
 1189 arguments in mind. Referring to the 2D case shown in Fig. 6a, we consider the effective
 1190 (travel time distribution) response, $h(t)$, to a rainfall pulse containing a chemical species over
 1191 the entire area of a catchment. Every point over this area may be considered a source of chemical
 1192 species (“tracer”). A stream running through the catchment acts as a line sink (collector) for
 1193 the tracer. This catchment picture can be idealised as two rectangles straddling this stream

1194 sink (Fig. 6a). Measurements of tracer arrivals at a control point downstream of this stream
 1195 (known as an “absorbing boundary”) yield a tracer arrival “counting rate” that is a
 1196 breakthrough curve.

1197 The first-passage time distribution $F(\mathbf{l}_s, t)$ defines the travel time distribution from a
 1198 (pulse) source at the origin \mathbf{l} to the point \mathbf{l}_s . Then the chemical tracer/species concentration at
 1199 position \mathbf{l}_s and time t , $c_s(\mathbf{l}_s, t)$ is given by

$$1200 \quad c_s(\mathbf{l}_s, t) = \int_0^\infty \sum_{\mathbf{l} \in \Omega} F(\mathbf{l}_s - \mathbf{l}, t') c_R(\mathbf{l}, t - t') dt' \quad (\text{Eq. 15})$$

1202 where $c_R(\mathbf{l}, t)$ is the chemical input from rainfall at a position \mathbf{l} in a catchment of area Ω .
 1203 Referring then to Fig. 6a, because we sample chemical arrivals downstream, we can consider
 1204 the sampling position as an “instantaneous” integration of all chemical species/tracer arrivals
 1205 from the catchment pathways along the entire length of the stream. Travel time within the
 1206 stream can generally be assumed negligible, relative to the catchment travel times, as stream
 1207 velocities are generally much faster than combined overland/subsurface flows. We thus
 1208 determine the total chemical flux into the stream by integrating over all chemical inputs in the
 1209 catchment that reach the stream; this defines overall first-passage time distributions at the
 1210 downstream measurement point. Assuming that all of the sampling positions in \mathbf{l}_s are small
 1211 regions compared to Ω , then $c_s(\mathbf{l}_s, t) \approx c_s$. For uniform rainfall distribution over Ω , we have
 1212 $c_R(\mathbf{l}, t) \approx c_R(t)$, and we can hence define for the effective, overall response (travel time
 1213 distribution)

$$1214 \quad h(t) \equiv \sum_{\mathbf{l} \in \Omega} F(\mathbf{l}, t) \quad (\text{Eq. 16})$$

1215
 1216 Long-term measurements of chloride tracer concentrations $c_R(t)$ in the rainfall over a
 1217 catchment area in Plynlimon, Wales, were compared to the time series of the chloride tracer
 1218 concentration $c_s(t)$ in the catchment Hafren stream (Kirchner et al., 2000). These authors
 1219 related the input and output concentrations through the convolution integral

$$1220 \quad c_s(t) = \int_0^\infty h(t') c_R(t - t') dt' \quad (\text{Eq. 17})$$

1222
 1223 Using a spectral analysis, Kirchner et al. (2000) concluded that overall chloride transport in
 1224 the catchment scaled as $h(t) \sim t^{-m}$, with $m \approx 0.5$, over a time period from 0.01 to 10 years.
 1225 They reported similar scaling in North American and Scandinavian field sites with $m \approx 0.4$ –
 1226 0.65.

1227
 1228 Kirchner et al. (2000) continued their analysis by noting (i) that an exponential travel time
 1229 distribution (which is implicit in the advection-dispersion equation; see discussion above Eq.
 1230 (11)) does not match the data, and (ii) that conceptualization of the entire catchment as a
 1231 single flow path, and use of the advection-dispersion equation to describe travel times, do not
 1232 correctly match even the basic character of the chloride concentration arrivals. The authors
 1233 concluded that catchment travel time distributions should be quantified as an approximate
 1234 power law distribution, to correctly account for long-time chemical retention and release in
 1235 catchments, and defined $h(t)$ as a gamma distribution (recall Eq. (14)). It should be recognised
 1236

1237 that the choice of a gamma distribution is empirical, and other functions can generate similar
 1238 behaviours in the spectral (Laplace or Fourier) domain. Significantly, the slope identified by
 1239 Kirchner et al. (2000) reflects high frequencies, i.e., short time scales; several decades of
 1240 tracer data to validate the power spectrum at low frequencies were not available.

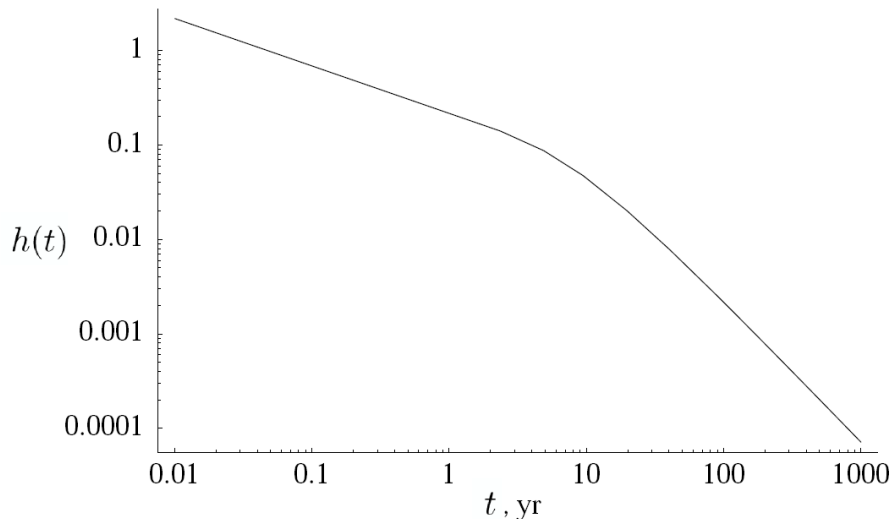
1241 Scher et al. (2002) reanalysed this catchment system behaviour with the CTRW
 1242 framework, arguing that subsurface flow and transport are dominant factors controlling the
 1243 overall chemical species arrival to the stream outlet measurement point. Based on Eqs. (15)
 1244 and (16), they first (re)examined the solution of the one-dimensional advection-dispersion
 1245 equation; they confirmed that the temporal dependence of $h(t)$ does not represent the field
 1246 measurements (similar to Kirchner et al., 2000). Significantly, though, they employed a pure
 1247 power law form of the transition time distribution, $\psi(t) \sim t^{-1-\beta}$, and developed Eqs. (15) and
 1248 (16) – based on the seminal analysis of Scher and Montroll (1975) – to obtain

$$1249 \quad h(t) \sim \begin{cases} t^{-1+\beta}, & t < t^* \\ t^{-1-\beta}, & t > t^* \end{cases} \quad \text{for } 0 < \beta < 1. \quad (\text{Eq. 18})$$

1251 The turnover time t^* between these two slopes arises naturally as an outcome of chemical
 1252 transport in the system embodied in Eq. (16). The smaller times represent chemical inputs
 1253 following along fastest flow paths to the sampling point; for $t > t^*$, all chemical inputs over
 1254 the entire catchment area are contributing particles to the sampling point, as accounted for in
 1255 Eq. (17). In this latter case, the power law represents the overall particle movement in the
 1256 domain, but especially the effects of the slow particles (longer transition times and influence
 1257 of less mobile zones) and the longer travel distances.

1259 In the context of the Hafren stream system, the turnover time t^* was estimated as about 10
 1260 years (Scher et al., 2002), in agreement with findings and measurement range of Kirchner et
 1261 al. (2000), with $\beta = 0.5$. Figure 8 shows a representative plot of Eq. (18) for this system. As
 1262 noted in Scher et al. (2002), it remains to analyse measurements to confirm the turnover to the
 1263 longer-time $t^{-1-\beta}$ scaling behaviour, which is indicative of extremely long retention times.
 1264 Note that high-resolution measurements of low concentration levels in water are generally
 1265 required to analyse these longer-time tails. The key recognition here is that while the effective
 1266 catchment response *may potentially*, initially (i.e., at relatively short times), be represented by
 1267 a type of gamma distribution (i.e., a power law $\sim t^{-1+\beta}$, ignoring the exponential cut-off) at
 1268 sufficiently small times (<10 years in the case of the Hafren catchment) – and this is
 1269 embodied in the CTRW framework as seen in Eq. (18) – full (CTRW framework) power law
 1270 behaviour (i.e., $\sim t^{-1-\beta}$) over longer times should also be incorporated to describe expected
 1271 long-term catchment retention behaviour. An evolution to Fickian transport, via an
 1272 exponential cut-off at very long times, can also be included (if relevant). To conclude, while
 1273 direct, quantitative application of CTRW to analysis of chemical transport at the catchment
 1274 scale remains to be done, it appears – on the basis of the conceptual pictures, extensive
 1275 application to subsurface systems and direct similarities to catchment systems, and the robust
 1276 and general nature of the CTRW formulation – to be a highly promising avenue for future
 1277 research.

1278



1279
 1280 **Figure 8** A log-log plot of $h(t)$ vs. t (after Scher et al., 2002; Copyright 2002, with permission
 1281 from the American Geophysical Union).
 1282

1283 4 CONCLUSIONS AND PERSPECTIVES

1284 4.1 Preferential flow and non-Gaussian travel times: The spatial and the 1285 temporal manifestation of organized complexity

1286
 1287 Based on Sects. 2 and 3, we can state that (a) preferential flow and related non-Fickian
 1288 transport is an omnipresent, unifying element between both water worlds, and (b) the CTRW
 1289 framework can effectively quantify and predict non-Fickian transport of water and chemicals
 1290 species in a manner that connects to and clearly steps beyond the advection-dispersion
 1291 paradigm. In this section, we link these insights to our central proposition that preferential
 1292 flow is a prime manifestation of how a local-scale heterogeneous flow process causes a
 1293 macroscale organised flow pattern in *space*. The key is to acknowledge that organisation
 1294 manifests also through organised dynamic behaviour in *time*, which occurs through non-
 1295 Fickian travel time distributions of water and chemical species. Note that the degree of
 1296 organisation in *space* manifests in the deviation of spatial patterns of system characteristics or
 1297 fluid flow from the maximum entropy pattern. The latter corresponds, in the case that the
 1298 mean value is known, to a uniform distribution of system characteristics and/or a uniform
 1299 flow pattern. Along the same lines, we propose that the degree of organisation in dynamic
 1300 behaviour in *time* manifests through the deviation of the breakthrough curve from the case of
 1301 a well-mixed Gaussian system, which is quantified within the CTRW framework based on the
 1302 power law exponent. A power law exponent ≥ 2 corresponds to well a mixed travel time
 1303 distribution. The latter reflect a spatial concentration equal to a Gaussian, which maximises
 1304 entropy when the *mean* and the *variance* are known (Trefry et al., 2003).

1305 In terms of how power law transition distributions are linked to the formation, evolution
 1306 and function of preferential flow paths in surface water systems, and how and if they can be
 1307 expected to improve representation thereof in models, we first emphasise that power law
 1308 transition time distributions are linked to the *function* of preferential flow paths, but not to

1309 their formation and evolution. It is clear and well-known that preferential flow implies non-
1310 Fickian residence times or travel distance. But what has not been recognized, though, is that
1311 the fingerprint of preferential flow in the overall travel time distribution can be captured by a
1312 (truncated) power law for the transition time distribution; and through the related exponent we
1313 can quantify the deviation from the well-mixed Fickian case. As discussed in Sect. 2.4, the
1314 findings of Edery et al. (2014) suggest a further connection between the characteristics of an
1315 aquifer and the power law exponent in breakthrough curves. This implies that the fitted
1316 parameters are a macroscale fingerprint of spatial media characteristics that determine the
1317 temporal arrival of chemical species. While we do not expect that this relation is unique, it
1318 does imply that “fitted” parameters have a physical meaning that can be used to constrain
1319 characteristics of the domain (i.e., the hydrological landscape mentioned above) in a spatially
1320 distributed model.

1321 We argue that this should also hold for other complex media characteristics that relate to
1322 their spatial organization, such as the correlation length or topology of preferential flow paths.
1323 We therefore suggest that these insights offer opportunities to relate signatures of spatial
1324 organization in flow patterns to signatures of temporal organization in breakthrough curves.
1325 For both perspectives, we can quantify organization using information entropy, as we showed
1326 in Sect. 2.4. These arguments might also offer, ultimately, opportunities to test whether
1327 hydrological systems and their preferential flow networks co-evolve towards more energy
1328 efficient drainage, which can also be quantified (Kleidon et al. 2013; Zehe et al., 2019;
1329 Savenije and Hrachowitz, 2017). We leave a more detailed reflection on this for future
1330 studies.

1331 **4.2 Overall conclusions and perspectives**

1332 In an effort to integrate and unify conceptualisation and quantitative modelling of the two
1333 “water worlds”– surface water and groundwater systems – we recognise preferential fluid
1334 flows as a unifying element and consider them as a manifestation of self-organisation.
1335 Preferential flows hinder perfect mixing within a system, due to a more “energy efficient” and
1336 hence faster throughput of water, which affects residence times of water, matter and chemical
1337 species in hydrological systems across all scales. While our main focus here is on the role of
1338 preferential flow for residence times and chemical transport, we relate our proposed unifying
1339 concept to role of preferential flow for energy conversions and energy dissipation associated
1340 with flows of water and mass.

1341 Essentially, we have proposed that related conceptualisations on the role of heterogeneity
1342 and preferential fluid flow for chemical species transport, and its quantitative characterisation,
1343 can be unified in terms of a theory, based on the CTRW framework, that connects these two
1344 water worlds in a dynamic framework. We emphasise the occurrence of power law
1345 behaviours that characterise travel times of chemical species, and highlight the critical role
1346 played by system heterogeneity and chemical species residence times, which are distinct from
1347 travel times of water. In particular, we compare and contrast specific power law distributions,
1348 and argue that the closely related inverse gamma and algebraic power law distributions are
1349 more appropriate than the oft-used gamma distribution to quantify chemical species transport.

1350 Moreover, we identify deviations from well-mixed Gaussian transport as a manifestation
1351 of self-organised dynamic behaviour in time, and the power law exponent as a suitable means

1352 to measure the strength of this deviation. Along a complementary line, we propose that self-
1353 organisation in space is immanent primarily through strongly localised preferential flow
1354 through rill and river networks at the land surface. We relate the degree of spatial organisation
1355 to the deviation of the flow pattern from spatially homogeneous flow, which is a state of
1356 maximum entropy. In this context, we reflect on the ongoing controversial discussion
1357 regarding whether or not self-organisation in open hydrological systems leads to evolution to
1358 a more energy efficient or even thermodynamic optimal system configuration. Finally, we
1359 propose that our concept of temporally organised travel times can help to test the possible
1360 emergence of thermodynamic optimality. Complementary to this idea, we suggest that an
1361 energetic perspective of chemical species transport may help to explain the organisation of
1362 travel paths (Fig. 4), in the sense that contrary to common assumptions, preferential pathways
1363 often include “bottlenecks” of low hydraulic conductivity. A testable option could be that
1364 chemical species travel along the path of maximum power, with power being defined in this
1365 case as flow of chemical energy (rather than flow of kinetic energy) through the system.

1366 Overall, we conclude that self-organisation arises equally in surface water and
1367 groundwater systems, as local heterogeneity and disorder in fluid flow and chemical transport
1368 processes lead to ordered behaviour at the macroscale. Naturally, the surface water
1369 community has developed a strong emphasis on the *localised spatial fingerprints*, because
1370 rills and rivers are clearly visible on land (Fig. 1), while the groundwater community has
1371 focused more naturally on *non-local temporal fingerprints*, as the flow paths are largely
1372 unobservable. But these are just two sides of the same conceptual picture of organised
1373 complexity (Dooge, 1986).

1374

1375 **Competing interests.** The authors declare that they have no conflict of interest.

1376

1377 **Acknowledgements.** The authors thank Markus Hrachowitz, Nicolas Rodriguez, Matthias
1378 Sprenger, and an anonymous referee for particularly constructive reviews of this work. B.B.
1379 gratefully acknowledges the support of research grants from the Israel Water Authority (Grant
1380 No. 45015199895) and the Israel Science Foundation (Grant No. 485/16); he thanks Harvey
1381 Scher for in-depth discussions. B.B. holds the Sam Zuckerberg Professorial Chair in
1382 Hydrology. E.Z. gratefully acknowledges intellectual support by the "Catchments as
1383 Organized Systems" (CAOS) research unit and funding of the German Research Foundation,
1384 DFG, (FOR 1598, ZE 533/11-1, ZE 533/12-1).

1385

1386 5 REFERENCES

- 1387 Abramowitz, M. and Stegun, I.: Handbook of Mathematical Functions, Dover, Mineola, N.Y.,
1388 1970.
- 1389 Angermann, L., Jackisch, C., Allroggen, N., Sprenger, M., Zehe, E., Tronicke, J., Weiler, M.,
1390 and Blume, T.: Form and function in hillslope hydrology: Characterization of subsurface
1391 flow based on response observations, Hydrology And Earth System Sciences, 21, 3727-
1392 3748, doi:10.5194/hess-21-3727-2017, 2017.

1393 Aronofsky, J. S. and Heller, J. P.: A diffusion model to explain mixing of flowing miscible
1394 fluids in porous media, *Trans. Am. Inst. Min. Metall. Pet. Eng.*, 210, 345-349, 1957.

1395 Bardossy, A.: Copula-based geostatistical models for groundwater quality parameters, *Water*
1396 *Resour. Res.*, 42, W11416, doi:10.1029/2005wr004754, 2006.

1397 Bardossy, A.: Calibration of hydrological model parameters for ungauged catchments,
1398 *Hydrol. Earth Syst. Sci.*, 11, 703-710, doi:10.5194/hess-11-703-2007, 2007.

1399 Bardossy, A. and Singh, S. K.: Robust estimation of hydrological model parameters, *Hydrol.*
1400 *Earth Syst. Sci.*, 12, 1273-1283, doi:10.5194/hess-12-1273-2008, 2008.

1401 Bejan, A., Lorente, S., and Lee, J.: Unifying constructal theory of tree roots, canopies and
1402 forests, *J. Theor. Biol.*, 254, 529-540, doi:10.1016/j.jtbi.2008.06.026, 2008.

1403 Benettin, P., Volkmann, T. H. M., von Freyberg, J., Frentress, J., Penna, D., Dawson, T. E.,
1404 and Kirchner, J.: Effects of climatic seasonality on the isotopic composition of evaporating
1405 soil waters, *Hydrol. Earth Syst. Sci.*, 22, 2881-2890, doi:10.5194/hess-22-2881-2018,
1406 2018.

1407 Ben-Zvi, R., Jiang, S., Scher, H., and Berkowitz, B.: Finite-Element Method solution of non-
1408 Fickian transport in porous media: The CTRW-FEM package, *Groundwater*, 57, 479-484,
1409 doi:10.1111/gwat.12813, 2019.

1410 Berkowitz, B. and Scher, H.: Exploring the nature of non-Fickian transport in laboratory
1411 experiments, *Adv. Water Resour.*, 32, 750-755, doi:10.1016/j.advwatres.2008.05.004,
1412 2009.

1413 Berkowitz, B., Cortis, A., Dentz, M., and Scher, H.: Modeling non-Fickian transport in
1414 geological formations as a continuous time random walk, *Rev. Geophys.*, 44, RG2003,
1415 doi:10.1029/2005RG000178, 2006.

1416 Berkowitz, B., Dror, I., Hansen, S. K., and Scher, H.: Measurements and models of reactive
1417 transport in geological media, *Rev. Geophys.*, 54, 930-986, doi:10.1002/2016RG000524,
1418 2016.

1419 Beven, K.: Changing ideas in hydrology - the case of physically-based models, *J. Hydrol.*,
1420 105, 157-172, doi:10.1016/0022-1694(89)90101-7, 1989.

1421 Beven, K. and Binley, A.: The future of distributed models: Model calibration and uncertainty
1422 prediction, *Hydrol. Proc.*, 6, 265-277, doi:10.1002/hyp.3360060305, 1992.

1423 Beven, K. and Germann, P.: Macropores and water flow in soils, *Water Resour. Res.*, 18,
1424 1311-1325, doi:10.1029/WR018i005p01311, 1982.

1425 Beven, K. and Germann, P.: Macropores and water flow in soils revisited, *Water Resour.*
1426 *Res.*, 49, 3071-3092, doi:10.1002/wrcr.20156, 2013.

1427 Bianchi, M., Zheng, C., Wilson, C., Tick, G. R., Liu, G., and Gorelick, S. M.: Spatial
1428 connectivity in a highly heterogeneous aquifer: From cores to preferential flow paths,
1429 *Water Resour. Res.*, 47, W05524, doi:10.1029/2009WR008966, 2011.

1430 Binet, F., Kersante, A., Munier-Lamy, C., Le Bayon, R. C., Belgly, M. J., and Shipitalo, M. J.:
1431 Lumbricid macrofauna alter atrazine mineralization and sorption in a silt loam soil, *Soil*
1432 *Biol. Biochem.*, 38, 1255-1263, doi:10.1016/j.soilbio.2005.09.018, 2006.

1433 Bishop, J. M., Callaghan, M. V., Cey, E. E., and Bentley, L. R.: Measurement and simulation
1434 of subsurface tracer migration to tile drains in low permeability, macroporous soil, *Water*
1435 *Resour. Res.*, 51(6), 3956-3981, doi:10.1002/2014WR016310, 2015.

- 1436 Blume, T., Zehe, E., and Bronstert, A.: Investigation of runoff generation in a pristine, poorly
 1437 gauged catchment in the Chilean Andes ii: Qualitative and quantitative use of tracers at
 1438 three spatial scales, *Hydrol. Proc.*, 22, 3676-3688, doi:10.1002/hyp.6970, 2008.
- 1439 Blume, T., Zehe, E., and Bronstert, A.: Use of soil moisture dynamics and patterns at different
 1440 spatio-temporal scales for the investigation of subsurface flow processes, *Hydrol. Earth
 1441 Syst. Sci.*, 13, 1215-1233, doi:10.5194/hess-13-1215-2009, 2009.
- 1442 Boano, F., Packman, A.I., Cortis, A., Revelli, R., and Ridolfi, L.: A continuous time random
 1443 walk approach to the stream transport of solutes, *Water Resour. Res.*, 43, W10425,
 1444 doi:10.1029/2007WR006062, 2007.
- 1445 Bodin, J.: From analytical solutions of solute transport equations to multidimensional time-
 1446 domain random walk (TDRW) algorithms, *Water Resour. Res.*, 51, 1860-1871,
 1447 doi:10.1002/2014WR015910, 2015.
- 1448 Bolduan, R. and Zehe, E.: Degradation of isoproturon in earthworm macropores and subsoil
 1449 matrix - a field study, *J. Plant Nutrition Soil Sci.*, 169, 87-94, doi:10.1002/jpin.200521754,
 1450 2006.
- 1451 Bonell, M., Pearce, A. J., and Stewart, M. K.: The identification of runoff-production
 1452 mechanisms using environmental isotopes in a tussock grassland catchment, eastern otago,
 1453 new-zealand, *Hydrol. Proc.*, 4, 15-34, doi:10.1002/hyp.3360040103, 1990.
- 1454 Botter G., Bertuzzo E., and Rinaldo A.: Transport in the hydrologic response: Travel time
 1455 distributions, soil moisture dynamics, and the old water paradox, *Water Resour. Res.*,
 1456 46(3), W03514, doi:10.1029/2009WR008371, 2010.
- 1457 Botter G., Bertuzzo E., and Rinaldo A.: Catchment residence and travel time distributions:
 1458 The master equation, *Geophys. Res. Lett.*, 38(11), L11403, doi:10.1029/2011GL047666,
 1459 2011.
- 1460 Bundt, M., Widmer, F., Pesaro, M., Zeyer, J., and Blaser, P.: Preferential flow paths:
 1461 Biological 'hot spots' in soils, *Soil Biol. Biochem.*, 33, 729-738, doi:10.1016/S0038-
 1462 0717(00)00218-2, 2001.
- 1463 Camporese, M., Paniconi, C., Putti, M., and Orlandini, S.: Surface-subsurface flow modeling
 1464 with path-based runoff routing, boundary condition-based coupling, and assimilation of
 1465 multisource observation data, *Water Resour. Res.*, 46, W0251210,
 1466 doi:1029/2008wr007536, 2010.
- 1467 Chabrier, G., Galactic stellar and substellar initial mass function, *Publ. Astron. Soc. Pac.* 115,
 1468 763-795, doi:10.1086/376392, 2003.
- 1469 Collins, R., Jenkins, A., and Harrow, M. A.: The contribution of old and new water to a storm
 1470 hydrograph determined by tracer addition to a whole catchment, *Hydrol. Processes*, 14,
 1471 701-711, doi:10.1002/(SICI)1099-1085(200003)14:43.0.CO;2-2, 2000.
- 1472 Cortis A. and Berkowitz B.: Computing "anomalous" contaminant transport in porous media:
 1473 The CTRW MATLAB toolbox, *Ground Water*, 43, 947-950, doi:10.1111/j.1745-
 1474 6584.2005.00045.x, 2005.
- 1475 Davies, J. and Beven, K.: Comparison of a multiple interacting pathways model with a
 1476 classical kinematic wave subsurface flow solution, *Hydrol. Sci. J.-J. Sci. Hydrol.*, 57, 203-
 1477 216, doi:10.1080/02626667.2011.645476, 2012.

1478 Davies, J., Beven, K., Rodhe, A., Nyberg, L., and Bishop, K.: Integrated modeling of flow
1479 and residence times at the catchment scale with multiple interacting pathways, *Water*
1480 *Resour. Res.*, 49, 4738-4750, doi:10.1002/wrcr.20377, 2013.

1481 Dentz, M., and Berkowitz, B.: Transport behavior of a passive solute in continuous time
1482 random walks and multirate mass transfer, *Water Resour. Res.*, 39, 1111,
1483 doi:10.1029/2001WR001163, 2003.

1484 Dentz, M., Cortis, A., Scher, H., and Berkowitz, B.: Time behavior of solute transport in
1485 heterogeneous media: Transition from anomalous to normal transport, *Adv. Water Resour.*,
1486 27(2), 155-173, doi:10.1016/j.advwatres.2003.11.002, 2004.

1487 Dentz, M., Scher, H., Holder, D., and Berkowitz, B.: Transport behaviour of coupled
1488 continuous-time random walks, *Phys. Rev. E*, 78, 41110,
1489 doi:10.1103/PhysRevE.78.041110, 2008.

1490 Dooge, J. C. I.: Looking for hydrological laws, *Water Resour. Res.*, 22, 46S-58S,
1491 doi:10.1029/WR022i09Sp0046S, 1986.

1492 Duan, Q. Y., Sorooshian, S., and Gupta, H.V.: Effective and efficient global optimization for
1493 conceptual rainfall-runoff models, *Water Resour. Res.*, 28, 1015-1031,
1494 doi:10.1029/91WR02985, 1992.

1495 Ebel, B. A., and Loague, K.: Physics-based hydrologic-response simulation: Seeing through
1496 the fog of equifinality, *Hydrol. Process.*, 20(13), 2887-2900, doi:10.1002/hyp.6388, 2006.

1497 Edery, Y., Guadagnini, A., Scher, H., and Berkowitz, B.: Origins of anomalous transport in
1498 disordered media: Structural and dynamic controls, *Water Resour. Res.*, 50, 1490-1505,
1499 doi:10.1002/2013WR015111, 2014.

1500 Everett, M. E.: *Near-Surface Applied Geophysics*, Cambridge University Press, Cambridge,
1501 2013.

1502 Ewen, J.: 'Samp' model for water and solute movement in unsaturated porous media involving
1503 thermodynamic subsystems and moving packets 1. Theory, *J. Hydrol.*, 182, 175-194,
1504 doi:10.1016/0022-1694(95)02925-7, 1996a.

1505 Ewen, J.: 'Samp' model for water and solute movement in unsaturated porous media involving
1506 thermodynamic subsystems and moving packets 2. Design and application, *J. Hydrol.*, 182,
1507 195-207, doi:10.1016/0022-1694(95)02926-5, 1996b.

1508 Faulkner, H.: Connectivity as a crucial determinant of badland morphology and evolution,
1509 *Geomorphology*, 100, 91-103, doi:10.1016/j.geomorph.2007.04.039, 2008.

1510 Fenicia, F., Kavetski, D., and Savenije, H. H. G.: Elements of a flexible approach for
1511 conceptual hydrological modeling: 1. Motivation and theoretical development, *Water*
1512 *Resour. Res.*, 47, W11510, doi:10.1029/2010wr010174, 2011.

1513 Fenicia, F., Kavetski, D., Savenije, H. H. G., Clark, M. P., Schoups, G., Pfister, L., and Freer,
1514 J.: Catchment properties, function, and conceptual model representation: Is there a
1515 correspondence?, *Hydrol. Proc.*, 28, 2451-2467, doi:10.1002/hyp.9726, 2014.

1516 Fenicia, F., Savenije, H. H. G., Matgen, P., and Pfister, L.: A comparison of alternative
1517 multiobjective calibration strategies for hydrological modelling. *Water Resour. Res.*, 43,
1518 W03434, doi:10.1029/2006WR005098, 2007.

1519 Feyen, L., Vazquez, R., Christiaens, K., Sels, O., and Feyen, J.: Application of a distributed
1520 physically-based hydrological model to a medium size catchment, *Hydrol. Earth Syst. Sci.*,
1521 4, 47-63, doi:10.5194/hess-4-47-2000, 2000.

1522 Flügel, W. A.: Delineating hydrological response units by geographical information system
1523 analyses for regional hydrological modelling using PRMS/MMS in the drainage basin of
1524 the River Bröl, Germany, *Hydrol. Process.*, 9, 423-436, doi:10.1002/hyp.3360090313,
1525 1995.

1526 Flury, M.: Experimental evidence of transport of pesticides through field soils - a review, *J.*
1527 *Environ. Qual.*, 25, 25-45, doi:10.2134/jeq1996.00472425002500010005x, 1996.

1528 Flury, M., Flühler, H., Leuenberger, J., and Jury, W. A.: Susceptibility of soils to preferential
1529 flow of water: A field study, *Water Resour. Res.*, 30, 1945-1954,
1530 doi:10.1029/94WR00871, 1994.

1531 Flury, M., Leuenberger, J., Studer, B., and Flühler, H.: Transport of anions and herbicides in a
1532 loamy and a sandy soil. , *Water Resour. Res.*, 31, 823-835, doi:10.1029/94WR02852,
1533 1995.

1534 Freeze, R. A. and Harlan, R. L.: Blueprint for a physically-based, digitally simulated
1535 hydrologic response model, *J. Hydrol.*, 9, 237-258, doi:10.1016/0022-1694(69)90020-1,
1536 1969.

1537 Gao, H., Hrachowitz, M., Fenicia, F., Gharari, S., and Savenije, H. H. G.: Testing the realism
1538 of a topography-driven model (flex-topo) in the nested catchments of the Upper Heihe,
1539 China, *Hydrol. Earth Syst. Sci.*, 18, 1895-1915, doi:10.5194/hess-18-1895-2014, 2014.

1540 Germann, P.: Preferential flow: Stokes approach to infiltration and drainage. *Geographica*
1541 *Bernensia*, doi:10.4480/GB2018.G88, 2018

1542 Gharari, S., Hrachowitz, M., Fenicia, F., and Savenije, H. H. G.: Hydrological landscape
1543 classification: Investigating the performance of hand based landscape classifications in a
1544 central european meso-scale catchment, *Hydrol. Earth Syst. Sci.*, 15, 3275-3291,
1545 doi:10.5194/hess-15-3275-2011, 2011.

1546 Goldstein, H.: *Classical Mechanics*, Pearson Education Limited, Harlow, U.K., 2013.

1547 Goller, R., Wilcke, W., Fleischbein, K., Valarezo, C., and Zech, W.: Dissolved nitrogen,
1548 phosphorus, and sulfur forms in the ecosystem fluxes of a montane forest in Ecuador.
1549 *Biogeochemistry*, 77, 57-89, doi:10.1007/s10533-005-1061-1, 2006.

1550 Gooseff, M. N., Wondzell, S. M., Haggerty, R., and Anderson, J.: Comparing transient
1551 storage modeling and residence time distribution (RTD) analysis in geomorphically varied
1552 reaches in the Lookout Creek basin, Oregon, USA, *Adv. Water Resour.*, 26(9), 925-937,
1553 doi:10.1016/S0309-1708(03)00105-2, 2003.

1554 Gouet-Kaplan, M. and Berkowitz, B.: Measurements of interactions between resident and
1555 infiltrating water in a lattice micromodel, *Vadose Zone J.*, 10, 624-633,
1556 doi:10.2136/vzj2010.0103, 2011.

1557 Grayson, R. B., Moore, I. D. and McMahon, T. A.: Physically based hydrologic modeling: 2.
1558 Is the concept realistic? *Water Resour. Res.*, 28(10), 2659-2666, doi:10.1029/92WR01259,
1559 1992.

1560 Gupta, H. V., Clark, M. P., Vrugt, J. A., Abramowitz, G. and Ye, M.: Towards a
1561 comprehensive assessment of model structural adequacy, *Water Resour. Res.*, 48(8), 1-16,
1562 doi:10.1029/2011WR011044, 2012.

1563 Haggerty, R. and Gorelick S. M.: Multiple rate mass transfer for modeling diffusion and
1564 surface reactions in media with pore-scale heterogeneity, *Water Resour. Res.*, 31(10),
1565 2383-2400, doi:10.1029/95WR10583, 1995.

- 1566 Haggerty, R., Wondzell, S. M., and Johnson, M. A.: Power-law residence time distribution in
 1567 the hyporheic zone of a 2nd-order mountain stream, *Geophys. Res. Lett.*, 29(13), 18-1-18-
 1568 4, doi:10.1029/2002GL014743, 2002.
- 1569 Haken, H.: *Synergetics: An introduction; nonequilibrium phase transitions and self-*
 1570 *organization in physics, chemistry and biology*, Springer Series in Synergetics, Springer
 1571 Berlin, 355 pp., 1983.
- 1572 Hammel, K. and Roth, K.: Approximation of asymptotic dispersivity of conservative solute in
 1573 unsaturated heterogeneous media with steady state flow, *Water Resour. Res.*, 34, 709-715,
 1574 doi:10.1029/98WR00004, 1998.
- 1575 Harman, C. J.: Time-variable transit time distributions and transport: Theory and application
 1576 to storage-dependent transport of chloride in a watershed, *Water Resour. Res.*, 51, 1-30,
 1577 doi:10.1002/2014wr015707, 2015.
- 1578 He, Y., Bardossy, A., and Zehe, E.: A review of regionalisation for continuous streamflow
 1579 simulation, *Hydrol. Earth Syst. Sci.*, 15, 3539-3553, doi:10.5194/hess-15-3539-2011,
 1580 2011a.
- 1581 He, Y., Bardossy, A., and Zehe, E.: A catchment classification scheme using local variance
 1582 reduction method, *J. Hydrol.*, 411, 140-154, doi:10.1016/j.jhydrol.2011.09.042, 2011b.
- 1583 Hergarten, S., Winkler, G., and Birk, S.: Transferring the concept of minimum energy
 1584 dissipation from river networks to subsurface flow patterns, *Hydrol. Earth Syst. Sci.*, 18,
 1585 4277-4288, doi:10.5194/hess-18-4277-2014, 2014.
- 1586 Hildebrandt, A., Kleidon, A., and Bechmann, M.: A thermodynamic formulation of root water
 1587 uptake, *Hydrol. Earth Syst. Sci.*, 20, 3441-3454, doi:10.5194/hess-20-3441-2016, 2016.
- 1588 Hoffman, F., Ronen, D., Pearl, Z.: Evaluation of flow characteristics of a sand column using
 1589 magnetic resonance imaging, *J. Contam. Hydrol.*, 22, 95-107, doi:10.1016/0169-
 1590 7722(95)00079-8, 1996.
- 1591 Hopp, L., and McDonnell, J. J.: Connectivity at the hillslope scale: Identifying interactions
 1592 between storm size, bedrock permeability, slope angle and soil depth, *J. Hydrol.*, 376(3-4),
 1593 378-391, doi:10.1016/j.jhydrol.2009.07.047, 2009.
- 1594 Howard, A. D.: Optimal angles of stream junctions: geometric stability to capture and
 1595 minimum power criteria, *Water Resour. Res.*, 7, 863-873, doi:10.1029/WR007i004p00863,
 1596 1971.
- 1597 Howard, A. D.: Theoretical model of optimal drainage networks, *Water Resour. Res.*, 26,
 1598 2107-2117, doi:10.1029/WR026i009p02107, 1990.
- 1599 Hrachowitz, M., and Clark, M. P.: HESS Opinions: The complementary merits of competing
 1600 modelling philosophies in hydrology, *Hydrol. Earth Syst. Sci.*, 21, 3953-3973,
 1601 doi:10.5194/hess-21-3953-2017, 2017.
- 1602 Hrachowitz, M., Benettin, P., van Breukelen, B. M., Fovet, O., Howden, N. J. K., Ruiz, L.,
 1603 van der Velde, Y., and Wade, A. J.: Transit times – the link between hydrology and water
 1604 quality at the catchment scale, *Wiley Interdisciplinary Reviews-Water*, 3, 629-657,
 1605 doi:10.1002/wat2.1155, 2016.
- 1606 Hrachowitz, M., Fovet, O., Ruiz, L., and Savenije, H. H.: Transit time distributions, legacy
 1607 contamination and variability in biogeochemical 1/f scaling: how are hydrological response
 1608 dynamics linked to water quality at the catchment scale? *Hydrol. Proc.*, 29(25), 5241-5256,
 1609 2015.

1610 Hrachowitz, M., Savenije, H., Boogard, T. A., Tetzlaff, D., and Soulsby, C.: What can flux
1611 tracking teach us about water age distribution patterns and their temporal dynamics?,
1612 *Hydrol. Earth Syst. Sciences*, 17, 533-564, doi:10.5194/hess-17-533-2013, 2013.

1613 Hrachowitz, M., Soulsby, C., Tetzlaff, D., Malcolm, I. A., and Schoups, G.: Gamma
1614 distribution models for transit time estimation in catchments: Physical interpretation of
1615 parameters and implications for time-variant transit time assessment, *Water Resour. Res.*,
1616 46, W10536, doi:10.1029/2010WR009148, 2010.

1617 Hundecha, Y. and Bardossy, A.: Modeling of the effect of land use changes on the runoff
1618 generation of a river basin through parameter regionalization of a watershed model, *J.*
1619 *Hydrol.*, 292, 281-295, doi:10.1016/j.jhydrol.2004.01.002, 2004.

1620 Jackisch, C. and Zehe, E.: Ecohydrological particle model based on representative domains,
1621 *Hydrol. Earth Syst. Sci.*, 22, 3639-3662, doi:10.5194/hess-22-3639-2018, 2018.

1622 Kapetas, L., Dror, I., and Berkowitz, B.: Evidence of preferential path formation and path
1623 memory effect during successive infiltration and drainage cycles in uniform sand columns,
1624 *J. Contam. Hydrol.*, 165, 1-10, doi:10.1016/j.jconhyd.2014.06.016., 2014.

1625 Kirchner, J. W.: A double paradox in catchment hydrology and geochemistry, *Hydrol. Proc.*,
1626 17, 871-874, doi: 10.1002/hyp.5108, 2003.

1627 Kirchner, J. W.: Aggregation in environmental systems – Part 1: Seasonal tracer cycles
1628 quantify young water fractions, but not mean transit times, in spatially heterogeneous
1629 catchments, *Hydrol. Earth Syst. Sciences*, 279-297, doi:10.5194/hess-20-279-2016, 2016.

1630 Kirchner, J. W., Feng, X., and Neal, C.: Fractal stream chemistry and its implications for
1631 contaminant transport in catchments, *Nature*, 403, 524-527, doi:10.1038/35000537, 2000.

1632 Klaus, J. and Zehe, E.: Modelling rapid flow response of a tile drained field site using a 2D-
1633 physically based model: Assessment of “equifinal” model setups, *Hydrol. Proc.*, 24, 1595-
1634 1609, doi:10.1002/hyp.7687, 2010.

1635 Klaus, J. and Zehe, E.: A novel explicit approach to model bromide and pesticide transport in
1636 connected soil structures, *Hydrol. Earth Syst. Sci.*, 15, 2127-2144, doi:10.5194/hess-15-
1637 2127-2011, 2011.

1638 Klaus, J., Zehe, E., Elsner, M., Kulls, C., and McDonnell, J. J.: Macropore flow of old water
1639 revisited: Experimental insights from a tile-drained hillslope, *Hydrol. Earth Syst. Sci.*, 17,
1640 103-118, doi:10.5194/hess-17-103-2013, 2013.

1641 Klaus, J., Zehe, E., Elsner, M., Palm, J., Schneider, D., Schroeder, B., Steinbeiss, S., van
1642 Schaik, L., and West, S.: Controls of event-based pesticide leaching in natural soils: A
1643 systematic study based on replicated field scale irrigation experiments, *J. Hydrol.*, 512,
1644 528-539, doi:10.1016/j.jhydrol.2014.03.020, 2014.

1645 Klaus, J., Chun, K. P., McGuire, K. J., and McDonnell, J. J.: Temporal dynamics of
1646 catchment transit times from stable isotope data, *Water Resour. Res.*, 51, 4208-4223,
1647 doi:10.1002/2014wr016247, 2015.

1648 Kleidon, A.: How does the earth system generate and maintain thermodynamic disequilibrium
1649 and what does it imply for the future of the planet?, *Philos. Trans. Royal Soc. A-Math.*
1650 *Phys. Eng. Sci.*, 370, 1012-1040, doi:10.1098/rsta.2011.0316, 2012a.

1651 Kleidon, A., Zehe, E., and Lin, H.: Thermodynamic limits of the critical zone and their
1652 relevance to hydrogeology, in: *Hydrogeology: Synergistic Integration of Soil Science*
1653 *and Hydrology*, 5 Elsevier, Amsterdam, 854 pp., p. 243, 2012b.

- 1654 Kleidon, A., Zehe, E., Ehret, U., and Scherer, U.: Thermodynamics, maximum power, and the
 1655 dynamics of preferential river flow structures at the continental scale, *Hydrol. Earth Syst.*
 1656 *Sci.*, 17, 225-251, doi:10.5194/hess-17-225-2013, 2013.
- 1657 Knudsen, J., Thomsen, A., and Refsgaard, J. C.: WATBAL, *Hydrol. Res.*, 17, 347-362,
 1658 doi.org/10.2166/nh.1986.0026, 1986.
- 1659 Koehler, B., Corre, M. D., Steger, K., Well, R., Zehe, E., Sueta, J. P., and Veldkamp, E.: An
 1660 in-depth look into a tropical lowland forest soil: Nitrogen-addition effects on the contents
 1661 of N₂O, CO₂ and CH₄ and N₂O isotopic signatures down to 2-m depth, *Biogeochemistry*,
 1662 111, 695-713, doi:10.1007/s10533-012-9711-6, 2012.
- 1663 Koehler, B., Zehe, E., Corre, M. D., and Veldkamp, E.: An inverse analysis reveals
 1664 limitations of the soil-CO₂ profile method to calculate CO₂ production and efflux for well-
 1665 structured soils, *Biogeosciences*, 7, 2311-2325, doi:10.5194/bg-7-2311-2010, 2010.
- 1666 Kondepudi, D., and Prigogine, I.: *Modern thermodynamics: From heat engines to dissipative*
 1667 *structures*, John Wiley Chichester, U.K., 1998.
- 1668 Lehmann, P., Hinz, C., McGrath, G., Tromp-van Meerveld, H. J., and McDonnell, J. J.:
 1669 Rainfall threshold for hillslope outflow: An emergent property of flow pathway
 1670 connectivity, *Hydrol. Earth Syst. Sci.*, 11, 1047-1063, doi:10.5194/hess-11-1047-2007,
 1671 2007.
- 1672 Levy, M. and Berkowitz, B.: Measurement and analysis of non-Fickian dispersion in
 1673 heterogeneous porous media, *J. Contam. Hydrol.*, 64(3-4), 203-226, doi:10.1016/S0169-
 1674 7722(02)00204-8, 2003.
- 1675 Lindstrom, G., Johansson, B., Persson, M., Gardelin, M., and Bergstrom, S.: Development
 1676 and test of the distributed HBV-96 hydrological model, *J. Hydrol.*, 201, 272-288,
 1677 doi:10.1016/S0022-1694(97)00041-3, 1997.
- 1678 Loritz, R., Hassler, S. K., Jackisch, C., Allroggen, N., van Schaik, L., Wienhöfer, J., and
 1679 Zehe, E.: Picturing and modeling catchments by representative hillslopes, *Hydrol. Earth*
 1680 *Syst. Sci.*, 21, 1225-1249, doi:10.5194/hess-21-1225-2017, 2017.
- 1681 Loritz, R., Gupta, H., Jackisch, C., Westhoff, M., Kleidon, A., Ehret, U., and Zehe, E.: On the
 1682 dynamic nature of hydrological similarity, *Hydrol. Earth Syst. Sci.*, 22, 3663-3684,
 1683 doi:10.5194/hess-22-3663-2018, 2018.
- 1684 Loritz, R., Kleidon, A., Jackisch, C., Westhoff, M., Ehret, U., Gupta, H., and Zehe, E.: A
 1685 topographic index explaining hydrological similarity by accounting for the joint controls of
 1686 runoff formation, *Hydrol. Earth Syst. Sci.*, 23, 3807-3821, doi:10.5194/hess-23-3807-2019,
 1687 2019.
- 1688 McDonnell, J. J.: The two water worlds hypothesis: Ecohydrological separation of water
 1689 between streams and trees?, *Wiley Interdisciplinary Reviews-Water*, 1, 323-329,
 1690 doi:10.1002/wat2.1027, 2014.
- 1691 McDonnell, J. J. and Beven, K.: Debates-the future of hydrological sciences: A (common)
 1692 path forward? A call to action aimed at understanding velocities, celerities and residence
 1693 time distributions of the headwater hydrograph, *Water Resour. Res.*, 50, 5342-5350,
 1694 doi:10.1002/2013wr015141, 2014.
- 1695 McGlynn, B. and Seibert, J.: Distributed assessment of contributing area and riparian
 1696 buffering along stream networks, *Water Resour. Res.*, 39, WR001521,
 1697 doi:10.1029/2002WR001521, 2003.

1698 McGlynn, B., McDonnell, J. J., Stewart, M., and Seibert, J.: On the relationships between
1699 catchment scale and streamwater mean residence time, *Hydrol. Proc.*, 17, 175-181,
1700 doi:10.1002/hyp.5085, 2002.

1701 McGrath, G. S., Hinz, C., and Sivapalan, M.: Modelling the impact of within-storm variability
1702 of rainfall on the loading of solutes to preferential flow pathways, *Eur. J. Soil Sci.*, 59, 24-
1703 33, doi:10.1111/j.1365-2389.2007.00987.x, 2008.

1704 McGrath, G. S., Hinz, C., Sivapalan, M., Dressel, J., Puetz, T., and Vereecken, H.: Identifying
1705 a rainfall event threshold triggering herbicide leaching by preferential flow, *Water Resour.*
1706 *Res.*, 46, W02513, doi:10.1029/2008wr007506, 2010.

1707 Mertens, J., Madsen, H., Feyen, L., Jacques, D., and Feyen, J.: Including prior information in
1708 the estimation of effective soil parameters in unsaturated zone modelling, *J. Hydrol.*, 294,
1709 251-269, doi:10.1016/j.jhydrol.2004.02.011, 2004.

1710 Milne, G.: Normal erosion as a factor in soil profile development. *Nature*, 138, 548-549,
1711 doi:10.1038/138548c0, 1936.

1712 Nash, J. E.: The form of the instantaneous unit hydrograph, IASH publication no. 45, 3-4,
1713 114-121, 1957.

1714 Niemi, A. J.: Residence time distribution of variable flow processes, *Int. J. Appl. Radiat. Isot.*,
1715 28, 855-860, doi:10.1016/0020-708X(77)90026-6, 1977.

1716 Nissan, A. and Berkowitz, B.: Anomalous transport dependence on Péclet number, porous
1717 medium heterogeneity, and a temporally varying velocity field, *Phys. Rev. E*, 99, 033108,
1718 doi:10.1103/PhysRevE.99.033108, 2019.

1719 Nissan, A., Dror, I., and Berkowitz, B.: Time-dependent velocity-field controls on anomalous
1720 chemical transport in porous media, *Water Resour. Res.*, 53, 3760-3769,
1721 doi:10.1002/2016WR020143, 2017.

1722 Oswald, S., Kinzelbach, W., Greiner, A., and Brix, G.: Observation of flow and transport
1723 processes in artificial porous media via magnetic resonance imaging in three dimensions,
1724 *Geoderma*, 80, 417-429, doi:10.1016/S0016-7061(97)00064-5, 1997.

1725 Paik, K. and Kumar, P.: Optimality approaches to describe characteristic fluvial patterns on
1726 landscapes, *Philos. Trans. R. Soc. B-Biol. Sci.*, 365, 1387-1395,
1727 doi:10.1098/rstb.2009.0303, 2010.

1728 Paltridge, G. W.: Climate and thermodynamic systems of maximum dissipation, *Nature*, 279,
1729 630-631, doi:10.1038/279630a0, 1979.

1730 Refsgaard, J. C. and Storm, B.: MikeShe, in: *Computer models of watershed hydrology*,
1731 edited by: Singh, V. P., Water Resources Publications, Highland Ranch, Colorado, USA,
1732 809-846, 1995.

1733 Reinhardt, L., and Ellis, M. A.: The emergence of topographic steady state in a perpetually
1734 dynamic self organised critical landscape, *Water Resour. Res.*, 51, 4986-5003,
1735 doi:10.1002/2014WR016223, 2015.

1736 Rinaldo, A., Maritan, A., Colaiori, F., Flammini, A., and Rigon, R.: Thermodynamics of
1737 fractal networks, *Phys. Rev. Lett.*, 76, 3364-3367, doi:10.1103/PhysRevLett.76.3364,
1738 1996.

1739 Rinaldo, A., Benettin, P., Harman, C. J., Hrachowitz, M., McGuire, K. J., van der Velde, Y.,
1740 Bertuzzo, E., and Botter, G.: Storage selection functions: A coherent framework for

1741 quantifying how catchments store and release water and solutes, *Water Resour. Res.*, 51,
1742 4840-4847, doi:10.1002/2015wr017273, 2015.

1743 Rodriguez, N. B., and Klaus, J.: Catchment travel times from composite storage selection
1744 functions representing the superposition of streamflow generation processes, *Water*
1745 *Resour. Res.*, 55, 9292-9314, doi:10.1029/2019wr024973, 2019.

1746 Rodriguez, N. B., McGuire, K. J., and Klaus, J.: Time-varying storage-water age relationships
1747 in a catchment with a mediterranean climate, *Water Resour. Res.*, 54, 3988-4008,
1748 doi:10.1029/2017wr021964, 2018.

1749 Rodriguez, N. B., Pfister, L., Zehe, E., and Klaus, J.: Testing the truncation of travel times
1750 with StorAge Selection functions using deuterium and tritium as tracers, *Hydrol. Earth*
1751 *Syst. Sci. Discuss.*, <https://doi.org/10.5194/hess-2019-501>, in review, 2019.

1752 Rodriguez-Iturbe, I. and Rinaldo, A.: *Fractal river basins: Chance and self-organization*,
1753 Cambridge Univ. Press, Cambridge U. K., 2001.

1754 Rodriguez-Iturbe, I., D'Odorico, P., Porporato, A., and Ridolfi, L.: On the spatial and
1755 temporal links between vegetation, climate, and soil moisture, *Water Resour. Res.*, 35,
1756 3709-3722, doi:10.1029/1999wr900255, 1999.

1757 Roth, K. and Hammel, K.: Transport of conservative chemical through an unsaturated two-
1758 dimensional Miller-similar medium with steady state flow, *Water Resour. Res.*, 32, 1653-
1759 1663, doi: 10.1029/96WR00756, 1996.

1760 Samaniego, L. and Bardossy, A.: Simulation of the impacts of land use/cover and climatic
1761 changes on the runoff characteristics at the mesoscale, *Ecol. Model.*, 196, 45-61,
1762 doi:10.1016/j.ecolmodel.2006.01.005, 2006.

1763 Sander, T. and Gerke, H. H.: Modelling field-data of preferential flow in paddy soil induced
1764 by earthworm burrows, *J. Contam Hydrol.*, 104, 126-136,
1765 doi:10.1016/j.jconhyd.2008.11.003, 2009.

1766 Savenije, H. H. G.: HESS Opinions "Topography driven conceptual modelling (FLEX-
1767 Topo)", *Hydrol. Earth Syst. Sci.*, 14, 2681-2692, doi:10.5194/hess-14-2681-2010, 2010.

1768 Savenije, H. H. G. and Hrachowitz, M.: HESS Opinions "Catchments as meta-organisms - a
1769 new blueprint for hydrological modelling", *Hydrol. Earth Syst. Sci.*, 21, 1107-1116,
1770 doi:10.5194/hess-21-1107-2017, 2017.

1771 Scheidegger, A. E.: An evaluation of the accuracy of the diffusivity equation for describing
1772 miscible displacement in porous media, *Proc. Theory Fluid Flow Porous Media 2nd Conf.*,
1773 101-116, 1959.

1774 Scher, H. and Montroll, E. W.: Anomalous transit time dispersion in amorphous solids, *Phys.*
1775 *Rev. B*, 12, 2455-2477, doi:10.1103/PhysRevB.12.2455, 1975.

1776 Scher, H., Margolin, G., Metzler, R., Klafter, J., and Berkowitz, B.: The dynamical foundation
1777 of fractal stream chemistry: The origin of extremely long retention times, *Geophys. Res.*
1778 *Let.*, 29(5), doi:10.1029/2001GL014123, 2002.

1779 Shannon, C. E.: A mathematical theory of communication, *Bell Syst. Tech.*, J. 27, 379-423.
1780 doi:10.1145/584091.584093, 1948.

1781 Sherman, L. K.: Streamflow from rainfall by the unit hydrograph method, *Eng. News Record*,
1782 180, 501-505, 1932.

1783 Simmons, C. S.: A stochastic-convective transport representation of dispersion in one
1784 dimensional porous media systems, *Water Resour. Res.*, 18, 1193-1214,
1785 doi:10.1029/WR018i004p01193, 1982.

1786 Šimunek, J., Jarvis, N. J., van Genuchten, M. T., and Gardenas, A.: Review and comparison
1787 of models for describing non-equilibrium and preferential flow and transport in the vadose
1788 zone, *J. Hydrol.*, 272, 14-35, doi:10.1016/S0022-1694(02)00252-4, 2003.

1789 Singh, S. K., McMillan, H., Bardossy, A., and Fateh, C.: Nonparametric catchment clustering
1790 using the data depth function, *Hydrol. Sci. J.-J. Sci. Hydrol.*, 61, 2649-2667,
1791 doi:10.1080/02626667.2016.1168927, 2016.

1792 Sivapalan, M.: From engineering hydrology to earth system science: Milestones in the
1793 transformation of hydrologic science, *Hydrol. Earth Syst. Sci.*, 22, 1665-1693, doi:
1794 doi:10.5194/hess-22-1665-2018, 2018.

1795 Sklash, M. G., and Farvolden, R. N.: The role of groundwater in storm runoff, *J. Hydrol.*, 43,
1796 45-65, doi: 10.1016/0022-1694(79)90164-1, 1979.

1797 Sklash, M. G., Beven, K. J., Gilman, K., and Darling, W. G.: Isotope studies of pipeflow at
1798 Plynlimon, Wales, UK, *Hydrol. Proc.*, 10, 921-944, doi:10.1002/(SICI)1099-
1799 1085(199607)10:7<921::AID-HYP347>3.0.CO;2-B, 1996.

1800 Sposito, G., Jury, W. A., and Gupta, V. K.: Fundamental problems in the stochastic
1801 convection-dispersion model of solute transport in aquifers and field soils, *Water Resour.*
1802 *Res.*, 22(1), 77-88, 1986.

1803 Sprenger, M., Tetzlaff, D., Buttle, J., Laudon, H., Leistert, H., Mitchell, C. P. J., Snelgrove, J.,
1804 Weiler, M., and Soulsby, C.: Measuring and modeling stable isotopes of mobile and bulk
1805 soil water, *Vadose Zone J.*, 17, 1-18, doi:10.2136/vzj2017.08.0149, 2018.

1806 Sternagel, A., Loritz, R., Wilcke, W., and Zehe, E.: Simulating preferential soil water flow
1807 and tracer transport using the Lagrangian Soil Water and Solute Transport Model, *Hydrol.*
1808 *Earth Syst. Sci.*, 23, 4249-4267, doi:10.5194/hess-23-4249-2019, 2019.

1809 Tromp-van Meerveld, H. J., and McDonnell, J. J.: Threshold relations in subsurface
1810 stormflow: 2. The fill and spill hypothesis, *Water Resour. Res.*, 42, W02411,
1811 doi:10.1029/2004wr003800, 2006.

1812 Turton, D. J., Barnes, D. R., and de Jesus Navar, J.: Old and new water in subsurface flow
1813 from a forest soil block, *J. Environ. Qual.*, 24, 139-146,
1814 doi:10.2134/jeq1995.00472425002400010020x, 1995.

1815 van der Velde, Y., Torfs, P. J. J. F., van der Zee, S. E. A. T. M., and Uijlenhoet, R.:
1816 Quantifying catchment scale mixing and its effect on time varying travel time distributions.
1817 *Water Resour. Res.*, 48, W06536, doi:10.1029/2011WR011310, 2012.

1818 van Schaik, L., Palm, J., Klaus, J., Zehe, E., and Schröder, B.: Linking spatial earthworm
1819 distribution to macropore numbers and hydrological effectiveness, *Ecohydrology*, 7, 401-
1820 408, doi:10.1002/eco.1358, 2014.

1821 Vogel, H. J. and Roth, K.: Quantitative morphology and network representation of soil pore
1822 structure, *Adv. Water Resour.*, 24, 233-242, doi:10.1016/S0309-1708(00)00055-5, 2001.

1823 Vogel, H. J., Cousin, I., Ippisch, O., and Bastian, P.: The dominant role of structure for solute
1824 transport in soil: Experimental evidence and modelling of structure and transport in a field
1825 experiment, *Hydrol. Earth Syst. Sci.*, 10, 495-506, doi:10.5194/hess10-495-2006, 2006.

1826 Vrugt, J. A. and Ter Braak, C. J. F.: Dream((d)): An adaptive markov chain monte carlo
1827 simulation algorithm to solve discrete, noncontinuous, and combinatorial posterior
1828 parameter estimation problems, *Hydrol. Earth Syst. Sci.*, 15, 3701-3713, doi:10.5194/hess-
1829 15-3701-2011, 2011.

1830 Wagener, T., and Wheater, H. S.: Parameter estimation and regionalization for continuous
1831 rainfall-runoff models including uncertainty, *J. Hydrol.*, 320, 132-154, 2006.

1832 Weiler, M., McGlynn, B. L., McGuire, K. J., and McDonnell, J. J.: How does rainfall become
1833 runoff? A combined tracer and runoff transfer function approach, *Water Resour. Res.*, 39,
1834 1315, doi:10.1029/2003wr002331, 2003.

1835 Weinberg, G. M. (1975). *An Introduction to General Systems Thinking*. New York: John
1836 Wiley & Sons, N.Y., p. 279.

1837 Westhoff, M. C. and Zehe, E.: Maximum entropy production: Can it be used to constrain
1838 conceptual hydrological models?, *Hydrol. Earth Syst. Sci.*, 17, 3141-3157,
1839 doi:10.5194/hess-17-3141-2013, 2013.

1840 Westhoff, M., Kleidon, A., Schymanski, S., Dewals, B., Nijse, F., Renner, M., Dijkstra, H.,
1841 Ozawa, H., Savenije, H., Dolman, H., Meesters, A., and Zehe, E.: ESD Reviews:
1842 Thermodynamic optimality in Earth sciences. The missing constraints in modeling Earth
1843 system dynamics? *Earth Syst. Dynam. Discuss.*, doi:10.5194/esd-2019-6, in review, 2019.

1844 Westhoff, M., Zehe, E., Archaubeau, P., and Dewals, B.: Does the Budyko curve reflect a
1845 maximum-power state of hydrological systems? A backward analysis, *Hydrol. Earth Syst.*
1846 *Sci.*, 20, 479-486, doi:10.5194/hess-20-479-2016, 2016.

1847 Wienhoefer, J. and Zehe, E.: Predicting subsurface stormflow response of a forested hillslope
1848 - the role of connected flow paths, *Hydrol. Earth Syst. Sci.*, 18, 121-138, doi:10.5194/hess-
1849 18-121-2014, 2014.

1850 Wienhofer, J., Germer, K., Lindenmaier, F., Farber, A., and Zehe, E.: Applied tracers for the
1851 observation of subsurface stormflow at the hillslope scale, *Hydrol. Earth Syst. Sci.*, 13,
1852 1145-1161, doi:10.5194/hess-13-1145-2009, 2009.

1853 Wilcke, W., Yasin, S., Valarezo, C., and Zech, W.: Change in water quality during the
1854 passage through a tropical montane rain forest in Ecuador. *Biogeochemistry* 55, 45-72,
1855 doi:10.1023/A:1010631407270, 2001.

1856 Winter, T. C.: The concept of hydrologic landscapes, *J. Am. Water Resour. Assoc.*, 37, 335-
1857 349, <https://doi.org/10.1111/j.1752-1688.2001.tb00973.x>. 2001.

1858 Worthington, S. R. H. and Ford D. C.: Self-organised permeability in carbonate aquifers,
1859 *Groundwater*, 47(3), 326-336, doi:10.1111/j.1745-6584.2009.00551.x, 2009.

1860 Wrede, S., Fenicia, F., Martinez-Carreras, N., Juilleret, J., Hissler, C., Krein, A., Savenije, H.
1861 H. G., Uhlenbrook, S., Kavetski, D., and Pfister, L.: Towards more systematic perceptual
1862 model development: A case study using 3 Luxembourgish catchments, *Hydrol. Proc.*, 29,
1863 2731-2750, doi:10.1002/hyp.10393, 2015.

1864 Zehe, E. and Jackisch, C.: A Lagrangian model for soil water dynamics during rainfall-driven
1865 conditions, *Hydrol. Earth Syst. Sci.*, 20, 3511-3526, doi:10.5194/hess-20-3511-2016, 2016.

1866 Zehe, E., Blume, T., and Blöschl, G.: The principle of 'maximum energy dissipation': A novel
1867 thermodynamic perspective on rapid water flow in connected soil structures, *Philos. Trans.*
1868 *R. Soc. B-Biol. Sci.*, 365, 1377-1386, doi:10.1098/rstb.2009.0308, 2010.

- 1869 Zehe, E., Ehret, U., Blume, T., Kleidon, A., Scherer, U., and Westhoff, M.: A thermodynamic
1870 approach to link self-organization, preferential flow and rainfall-runoff behaviour, *Hydrol.*
1871 *Earth Syst. Sci.*, 17, 4297-4322, doi:10.5194/hess-17-4297-2013, 2013.
- 1872 Zehe, E., Ehret, U., Pfister, L., Blume, T., Schroder, B., Westhoff, M., Jackisch, C.,
1873 Schymanski, S. J., Weiler, M., Schulz, K., Allroggen, N., Tronicke, J., van Schaik, L.,
1874 Dietrich, P., Scherer, U., Eccard, J., Wulfmeyer, V., and Kleidon, A.: Hess opinions: From
1875 response units to functional units: A thermodynamic reinterpretation of the hru concept to
1876 link spatial organization and functioning of intermediate scale catchments, *Hydrol. Earth*
1877 *Syst. Sci.*, 18, 4635-4655, doi:10.5194/hess-18-4635-2014, 2014.
- 1878 Zehe, E., Loritz, R., Jackisch, C., Westhoff, M., Kleidon, A., Blume, T., Hassler, S. K., and
1879 Savenije, H. H.: Energy states of soil water – a thermodynamic perspective on soil water
1880 dynamics and storage-controlled streamflow generation in different landscapes, *Hydrol.*
1881 *Earth Syst. Sci.*, 23, 971-987, doi:10.5194/hess-23-971-2019, 2019.
- 1882 Zhang, Y., Benson, D. A., and Reeves, D. M.: Time and space nonlocalities underlying
1883 fractional-derivative models: Distinction and review of field applications, *Adv. Water*
1884 *Resour.*, 32, 561-581, doi:10.1016/j.advwatres.2009.01.008, 2009.